

Solution of a Braneworld Big Crunch/Big Bang Cosmology

Paul L. McFadden* and Neil Turok†

*DAMTP, Center for Mathematical Sciences,
Wilberforce Road, Cambridge, CB3 0WA, UK.*

Paul J. Steinhardt‡

*Joseph Henry Laboratories, Princeton University,
Princeton, New Jersey 08544, USA.*

(Dated: 11th February 2019)

Abstract

We solve for the cosmological perturbations in a five-dimensional background consisting of two separating or colliding boundary branes, as an expansion in the collision speed V divided by the speed of light c . Our solution permits a detailed check of the validity of four-dimensional effective theory in the vicinity of the event corresponding to the big crunch/big bang singularity. We show that the four-dimensional description fails at the first nontrivial order in $(V/c)^2$. At this order, there is nontrivial mixing of the two relevant four-dimensional perturbation modes (the growing and decaying modes) as the boundary branes move from the narrowly-separated limit described by Kaluza-Klein theory to the well-separated limit where gravity is confined to the positive-tension brane. We comment on the cosmological significance of the result and compute other quantities of interest in five-dimensional cosmological scenarios.

*Electronic address: p.l.mcfadden@damtp.cam.ac.uk

†Electronic address: n.g.turok@damtp.cam.ac.uk

‡Electronic address: steinh@princeton.edu

I. INTRODUCTION

One of the most striking implications of string theory and M theory is that there are extra spatial dimensions whose size and shape determine the particle spectrum and couplings of the low energy world. If the extra dimensions are compact and of fixed size R , their existence results in a tower of Kaluza-Klein massive modes whose mass scale is set by R^{-1} . Unfortunately, this prediction is hard to test if the only energy scales accessible to experiment are much lower than R^{-1} . At low energies, the massive modes decouple from the low energy effective theory and are, for all practical purposes, invisible. Therefore, we have no means of checking whether the four-dimensional effective theory observed to fit particle physics experiments is actually the outcome of a simpler higher-dimensional theory.

The one situation where the extra dimensions seem bound to reveal themselves is in cosmology. At the big bang, the four-dimensional effective theory (Einstein gravity or its stringy generalization) breaks down, indicating that it must be replaced by an improved description. There are already suggestions of improved behavior in higher-dimensional string and M theory. If matter is localized on two boundary branes, the matter density remains finite at a brane collision even though this moment is, from the perspective of the four-dimensional effective theory, the big bang singularity [1, 2, 3]. Likewise, the equations of motion for fundamental strings are actually regular at $t = 0$ in string theory, in the relevant background solutions [4].

In this paper, we shall not study the singularity itself. Instead, we will study the behavior of higher-dimensional gravity as the universe emerges from a brane collision. Our particular concern is to determine the extent to which the four-dimensional effective theory accurately captures the higher-dimensional dynamics near the big bang singularity.

The model we study is the simplest possible model of braneworld gravity. It consists of two empty Z_2 -branes (or orbifold planes) of opposite tension separated by a five-dimensional bulk with negative cosmological constant, corresponding to an anti-de Sitter (AdS) radius L [5]. Many works have been devoted to obtaining exact or approximate solutions for this model, for static or moving branes [6, 7, 8]. Our methods have much in common with these earlier works, in particular the idea that, when the branes move slowly, the four-dimensional effective theory works well. However, our focus and goals are rather different.

When the two boundary branes are very close to one another, the warping of the five-

dimensional bulk and the tension of the branes become irrelevant. In this situation, the low energy modes of the system are well-described by a simple Kaluza-Klein reduction from five to four dimensions, *i.e.*, gravity plus a scalar field (the Z_2 projections eliminate the gauge field zero mode). We shall verify this expectation. However, when the two branes are widely separated, the physics is quite different. In this regime, the warping of the bulk plays a key role, causing the low energy gravitational modes to be localized on the positive-tension brane [9, 10, 11]. The four-dimensional effective theory describing this new situation is nevertheless identical, consisting of Einstein gravity and a scalar field, the radion, describing the separation of the two branes.

In this paper, we study the transition between these two regimes – from the naive Kaluza-Klein reduction to localized Randall-Sundrum gravity – at finite brane speed. In the two asymptotic regimes – the narrowly-separated brane limit and the widely-separated limit – the cosmological perturbation modes show precisely the behavior predicted by the four-dimensional effective theory. There are two massless scalar perturbation modes; in longitudinal gauge, and in the long wavelength ($k \rightarrow 0$) limit, one mode is constant and the other decays as t_4^{-2} , where t_4 is the conformal time. In the four-dimensional description, these two perturbation modes are entirely distinct: one is the curvature perturbation mode; the other is a local time delay to the big bang. However, we shall show that in the five-dimensional theory, at first nontrivial order in the speed of the brane collision, the two modes mix. If, for example, one starts out in the time delay mode at small t_4 , one ends up in a mixture of the time delay and curvature perturbation modes as $t_4 \rightarrow \infty$. Thus the two cosmological perturbation modes – the growing and decaying adiabatic modes – mix in the higher-dimensional braneworld setup, a phenomenon which is prohibited in four dimensions.

The mode-mixing occurs as a result of the qualitative change in the nature of the low energy modes of the system. At small brane separations the low energy modes are nearly uniform across the extra dimension. Yet as the brane separation becomes larger than the bulk warping scale, the low energy modes become exponentially localized on the positive-tension brane. If the branes separate at finite speed, the localization process fails to keep pace with the brane separation and the low energy modes do not evolve adiabatically. Instead, they evolve into a mixture involving higher Kaluza-Klein modes, and the four-dimensional effective description fails.

As mentioned, the mixing we see between the two scalar perturbation modes would be

prohibited in any local four-dimensional effective theory consisting of Einstein gravity and matter fields, no matter what the matter fields were. Therefore the mixing is a truly five-dimensional phenomenon, which cannot be modeled with a local four-dimensional effective theory. There is an independent argument against the existence of any local four-dimensional description of these phenomena. In standard Kaluza-Klein theory, it is well known that the entire spectrum of massive modes is actually spin two [12]. Yet, despite many attempts, no satisfactory Lagrangian description of massive, purely spin two fields has ever been found [13, 14]. Again, this suggests that one should not expect to describe the excitation of the higher Kaluza-Klein modes in terms of an improved, local, four-dimensional effective theory.

The system we study consists of two branes emerging from a collision. In this situation, there are important simplifications which allow us to specify initial data rather precisely. When the brane separation is small, the fluctuation modes neatly separate into light Kaluza-Klein zero modes, which are constant along the extra dimension, and massive modes with nontrivial extra-dimensional dependence. Furthermore, the brane tensions and the bulk cosmological constant become irrelevant at short distances. It is thus natural to specify initial data which map precisely onto four-dimensional fields in the naive dimensionally-reduced theory describing the limit of narrowly-separated branes. With initial data specified this way, there are no ambiguities in the system. The two branes provide boundary conditions for all time and the five-dimensional Einstein equations yield a unique solution, for arbitrary four-dimensional initial data.

Our main motivation is the study of cosmologies in which the big bang was a brane collision, such as the cyclic model [1]. Here, a period of dark energy domination, followed by slow contraction of the fifth dimension, renders the branes locally flat and parallel at the collision. During the slow contraction phase, growing, adiabatic, scale-invariant perturbations are imprinted on the branes prior to the collision. However, if the system is accurately described by four-dimensional effective theory throughout, then, as a number of authors have noted [15, 16, 17, 18, 19, 20], there is an apparent roadblock to the passage of the scale-invariant perturbations across the bounce. Namely, it is hard to see how the growing mode in the contracting phase, usually described as a local time delay, could match onto the growing mode in the expanding phase, usually described as a curvature perturbation. In this paper, we show that the four-dimensional effective theory fails at order $(V/c)^2$, where V is the collision speed and c is the speed of light. The four-dimensional description works

well when the branes are close together, or far apart. However, as the branes move from one regime to the other, the two four-dimensional modes mix in a nontrivial manner.

The mixing we find is an explicit demonstration of a new physical principle: namely, the approach of two boundary branes along a fifth dimension produces physical effects that cannot properly be modeled by a local four-dimensional effective theory. In this paper, we deal with the simplest case involving two empty boundary branes separated by a bulk with a negative cosmological constant. For the cyclic model, the details are more complicated [21]. The bulk possesses an additional bulk stress ΔT_5^5 , associated with the inter-brane force, that plays a vital role in converting a growing mode corresponding to a pure time delay perturbation into a mixture of time delay and curvature modes on the brane. We also explain how subsequent five-dimensional effects cause the curvature on the brane to feed into the adiabatic growing mode perturbation in the four-dimensional effective theory after the bang. The details are different, but the general principle is the same as in the case considered in this paper. One must go beyond the four-dimensional effective theory and consider the full five-dimensional theory to compute properly the evolution of perturbations before and after a brane collision.

Even though our main concern is with cyclic/ekpyrotic models, our methods are likely to be more broadly applicable in braneworld models. (See *e.g.* [22, 23, 24] for reviews). Our methods may be extended, for example, to models with better motivation from fundamental theory, such as heterotic M theory [25, 26]. One may also include matter on the branes. Another interesting application would be to study the evolution of a four-dimensional black hole in the limit of narrowly-separated branes, *i.e.*, a black string, as the two branes separate and the Gregory-Laflamme instability appears.

The outline of this paper is as follows. In Section II we provide an overview of our three solution methods. In Section III we solve for the background and cosmological perturbations using a series expansion in time about the collision. In Section IV we present an improved method in which the dependence on the fifth dimension is approximated using a set of higher-order Dirichlet or Neumann polynomials. In Section V we develop an expansion about the small- (V/c) scaling solution, before comparing our results with those of the four-dimensional effective theory in Section VI. We conclude with a discussion of mode-mixing in Section VII. Detailed explicit solutions may be found in the Appendices, and the Mathematica code implementing our calculations is available online [27].

II. THREE SOLUTION METHODS

In this section, we review the three solution methods employed, noting their comparative merits. For the model considered here, with no dynamical bulk fields, there is a Birkhoff-like theorem guaranteeing the existence of coordinates in which the bulk is static. It is easy to solve for the background in these coordinates. However, the motion of the branes complicates the Israel matching conditions rendering the treatment of perturbations difficult. It is preferable to choose a coordinate system in which the branes are located at fixed spatial coordinate $y = \pm y_0$, and the bulk evolves with time.

We shall employ a coordinate system in which the five-dimensional line element for the background takes the form

$$ds^2 = n^2(t, y)(-dt^2 + t^2 dy^2) + b^2(t, y)d\vec{x}^2, \quad (1)$$

where y parameterizes the fifth dimension and x^i , $i = 1, 2, 3$, the three noncompact dimensions. Cosmological isotropy excludes $dt dx^i$ or $dy dx^i$ terms, and homogeneity ensures n and b are independent of \vec{x} . The t, y part of the background metric may then be taken to be conformally flat. One can write the metric for two-dimensional Minkowski spacetime in Milne form so that the branes are located at $y = \pm y_0$ and collide at $t = 0$. By expressing the metric in locally Minkowski coordinates, $T = t \cosh y$ and $Y = t \sinh y$, one sees that the collision speed is $(V/c) = \tanh 2y_0$ and the relative rapidity of the collision is $2y_0$. As long as the bulk metric is regular at the brane collision and possesses cosmological symmetry, the line element may always be put into the form (1). Furthermore, by suitably rescaling coordinates one can choose $b(0, y) = n(0, y) = 1$.

In order to describe perturbations about this background, one needs to specify an appropriate gauge choice. Five-dimensional longitudinal gauge is particularly convenient [28]: firstly, it is completely gauge-fixed; secondly, the brane trajectories are unperturbed in this gauge [29], so that the Israel matching conditions are relatively simple; and finally, in the absence of anisotropic stresses, the traceless part of the Einstein G_j^i (spatial) equation yields a constraint amongst the perturbation variables, reducing them from four to three. In light of these advantages, we will work in five-dimensional longitudinal gauge for the entirety of this paper.

Our three solution methods are as follows:

- **Series expansion in t**

The simplest solution method for the background is to solve for the metric functions $n(t, y)$ and $b(t, y)$ as a series in powers of t about $t = 0$. At each order, the bulk Einstein equations yield a set of ordinary differential equations in y , with the boundary conditions provided by the Israel matching conditions. These are straightforwardly solved. A similar series approach, involving powers of t and powers of t times $\ln t$ suffices for the perturbations.

The series approach is useful at small times $(t/L) \ll 1$ since it provides the precise solution for the background plus generic perturbations, close to the brane collision, for all y and for any collision rapidity y_0 . It allows one to uniquely specify four-dimensional asymptotic data as t tends to zero. However, the series thus obtained fails to converge at quite modest times. Following the system to long times requires a more sophisticated method. Instead of taking (t/L) as our expansion parameter, we want to use the dimensionless rapidity of the brane collision y_0 , and solve at each order in y_0 .

- **Expansion in Dirichlet/Neumann polynomials in y**

In this approach we represent the spacetime metric in terms of variables obeying either Dirichlet or Neumann boundary conditions on the branes. We then express these variables as series of Dirichlet or Neumann polynomials in y and y_0 , bounded at each subsequent order by an increasing power of the collision rapidity y_0 . (Recall that the range of the y coordinate is bounded by $|y| \leq y_0$). The coefficients in these expansions are undetermined functions of t . By solving the five-dimensional Einstein equations perturbatively in y_0 , we obtain a series of ordinary differential equations in t , which can then be solved exactly. In this Dirichlet/Neumann polynomial expansion, the Israel boundary conditions on the branes are satisfied automatically at every order in y_0 , while the initial data at small t are provided by the previous series solution method.

The Dirichlet/Neumann polynomial expansion method yields simple, explicit solutions for the background and perturbations as long as (t/L) is smaller than $1/y_0$. Since $y_0 \ll 1$, this considerably improves upon the naive series expansion in t . However, for (t/L) of order $1/y_0$, the expansion fails because the growth in the coefficients overwhelms the extra powers of y_0 at successive orders. Since $(t/L) \sim 1/y_0$ corresponds to brane separations of order the AdS radius, the Dirichlet/Neumann polynomial expansion method fails to describe the late-time behavior of the system, and a third method is needed.

- **Expansion about the scaling solution**

The idea of our third method is to start by identifying a scaling solution, whose form is independent of y_0 for all $y_0 \ll 1$. This scaling solution is well-behaved for all times and therefore a perturbation expansion in y_0 about this solution is similarly well-behaved, even at very late times. To find the scaling solution, we first change variables from t and y to an equivalent set of dimensionless variables. The characteristic velocity of the system is the brane speed at the collision, $V = c \tanh 2y_0 \sim 2cy_0$, for small y_0 , where we have temporarily restored the speed of light c . Thus we have the dimensionless time parameter $x = y_0 ct/L \sim Vt/L$, of order the time for the branes to separate by one AdS radius. We also rescale the y -coordinate by defining $\omega = y/y_0$, whose range is $-1 \leq \omega \leq 1$, independent of the characteristic velocity.

As we shall show, when re-expressed in these variables, for small y_0 , the bulk Einstein equations become perturbatively *ultralocal*: at each order in y_0 one only has to solve an ordinary differential equation in ω , with a source term determined by time derivatives of lower order terms. The original partial differential equations reduce to an infinite series of ordinary differential equations in ω which are then easily solved order by order in y_0 .

This method, an expansion in y_0 about the scaling solution, is the most powerful and may be extended to arbitrarily long times t and for all brane separations. As is well known for this model, a Birkhoff-like theorem holds for backgrounds with cosmological symmetry. The bulk in between the two branes is just a slice of five-dimensional Schwarzschild-AdS spacetime [22, 23, 24] within which the two branes move, with a virtual black hole lying outside of the physical region, beyond the negative-tension brane. As time proceeds, the negative-tension brane becomes closer and closer to the horizon of the Schwarzschild-AdS black hole. Even though its location in the Birkhoff-frame (static) coordinates freezes (see Figure 1), its proper speed grows and the y_0 expansion fails. Nonetheless, by analytic continuation of our solution in ω and x , we are able to circumvent this temporary breakdown of the y_0 expansion and follow the positive-tension brane, and the perturbations localized near it, as they run off to the boundary of anti-de Sitter spacetime.

Our expansion about the scaling solution is closely related to derivative-expansion techniques developed earlier by a number of authors [6, 7, 8]. In these works, an expansion in terms of brane curvature over bulk curvature was used. For cosmological solutions, this is

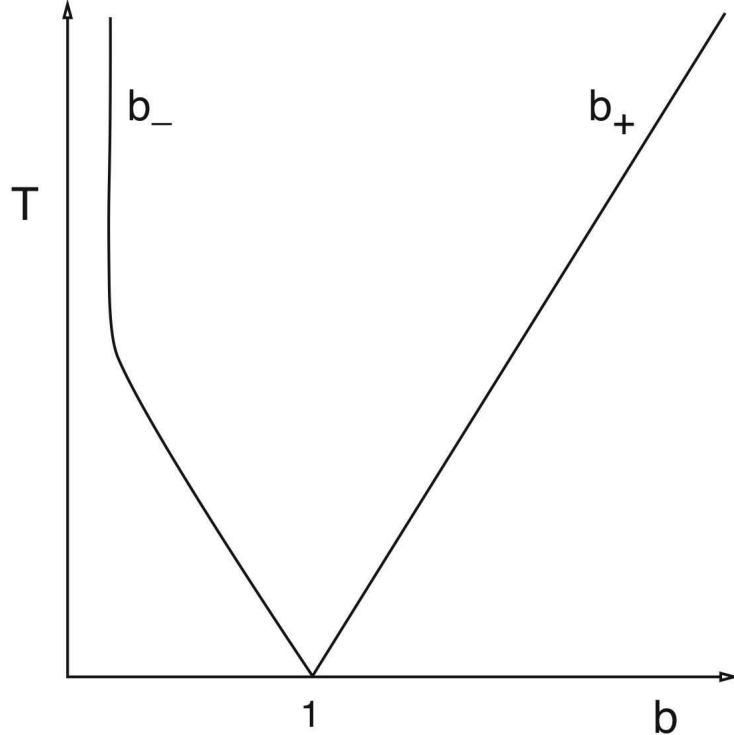


Figure 1: The background brane scale factors b_{\pm} plotted as a function of the Birkhoff-frame time T , where b_{\pm} have been normalized to unity at $T = 0$. In these coordinates the bulk is Schwarzschild-AdS: the brane trajectories are then determined by integrating the Israel matching conditions, given in Appendix E. In the limit as $T \rightarrow \infty$, the negative-tension brane asymptotes to the event horizon of the black hole, while the positive-tension brane asymptotes to the boundary of AdS.

equivalent to an expansion in $L\mathcal{H}^+$, where \mathcal{H}^+ is the Hubble constant on the positive-tension brane. However, we specifically want to study the time-dependence of the perturbations for all times from the narrowly-separated to the well-separated brane limit. For this purpose it is better to use a time-independent expansion parameter (y_0) and to include all the appropriate time-dependence order by order in the expansion.

Moreover, in the earlier works, the goal was to find the four-dimensional effective description more generally, without specifying that the branes emerged from a collision with perturbations in the lowest Kaluza-Klein modes. Consequently, the solutions obtained contained a number of undetermined functions. In the present context, however, the initial conditions along the extra dimension are completely specified close to the brane collision

by the requirement that only the lowest Kaluza-Klein modes be excited. The solutions we obtain here are fully determined, with no arbitrary functions entering our results.

Returning to the theme of the four-dimensional effective theory, we expect on general grounds that this should be valid in two particular limits: firstly, as we have already discussed, a Kaluza-Klein description will apply at early times near to the collision, when the separation of the branes is much less than L . Here, the warping of the bulk geometry and the brane tensions can be neglected. Secondly, when the branes are separated by many AdS lengths, one expects gravity to become localized on the positive-tension brane, which moves ever more slowly as time proceeds, so the four-dimensional effective theory should become more and more accurate.

Equipped with our five-dimensional solution for the background and perturbations obtained by expanding about the scaling solution, we find ourselves able to test the four-dimensional effective theory explicitly. We will show that the four-dimensional effective theory accurately captures the five-dimensional dynamics to leading order in the y_0 -expansion, but fails at the first nontrivial order. Our calculations reveal that the four-dimensional perturbation modes undergo a mixing in the transition between the Kaluza-Klein effective theory at early times and the brane-localized gravity at late times. This effect is a consequence of the momentary breakdown of the effective theory when the brane separation is of the order of an AdS length, and cannot be seen from four-dimensional effective theory calculations alone.

III. SERIES SOLUTION IN t

As described above, we find it simplest to work in coordinates in which the brane locations are fixed but the bulk evolves. The bulk metric is therefore given by (1), with the brane locations fixed at $y = \pm y_0$ for all time t . The five-dimensional solution then has to satisfy both the Einstein equations and the Israel matching conditions on the branes [30].

The bulk Einstein equations read $G_\mu^\nu = -\Lambda\delta_\mu^\nu$, where the bulk cosmological constant is $\Lambda = -6/L^2$ (we work in units in which the four-dimensional gravitational coupling $8\pi G_4 = 8\pi G_5/L = 1$). Evaluating the linear combinations $G_0^0 + G_5^5$ and $G_0^0 + G_5^5 - (3/2)G_i^i$ (where 0 denotes time, 5 labels the y direction, and i denotes one of the noncompact directions, with

no sum implied), we find:

$$\beta_{,\tau\tau} - \beta_{,yy} + \beta_{,\tau}^2 - \beta_{,y}^2 + 12e^{2\nu} = 0 \quad (2)$$

$$\nu_{,\tau\tau} - \nu_{,yy} + \frac{1}{3}(\beta_{,y}^2 - \beta_{,\tau}^2) - 2e^{2\nu} = 0, \quad (3)$$

where $(t/L) = e^\tau$, $\beta \equiv 3 \ln b$ and $\nu \equiv \ln(nt/L)$. The Israel matching conditions on the branes read [28, 29]

$$\frac{b_{,y}}{b} = \frac{n_{,y}}{n} = \frac{nt}{L}, \quad (4)$$

where all quantities are to be evaluated at the brane locations, $y = \pm y_0$.

We will begin our assault on the bulk geometry by constructing a series expansion in t about the collision, implementing the Israel matching conditions on the branes at each order in t . This series expansion in t is then exact in both y and the collision rapidity y_0 . Its chief purpose will be to provide initial data for the more powerful solution methods that we will develop in the following sections.

The Taylor series solution in t for the background was first presented in [29]:

$$n = 1 + (\operatorname{sech} y_0 \sinh y) \frac{t}{L} + \frac{1}{4} \operatorname{sech}^2 y_0 (-3 + 2 \cosh 2y + \cosh 2y_0) \frac{t^2}{L^2} + O\left(\frac{t^3}{L^3}\right) \quad (5)$$

$$b = 1 + (\operatorname{sech} y_0 \sinh y) \frac{t}{L} + \frac{1}{2} \operatorname{sech}^2 y_0 (\cosh 2y - \cosh 2y_0) \frac{t^2}{L^2} + O\left(\frac{t^3}{L^3}\right). \quad (6)$$

(Note that in the limit as $t \rightarrow 0$ we correctly recover compactified Milne spacetime).

Here, however, we will need the perturbations as well. Working in five-dimensional longitudinal gauge for the reasons given in the previous section, the perturbed bulk metric takes the form (see Appendix A)

$$ds^2 = n^2 \left(-(1 + 2\Phi_L) dt^2 - 2W_L dt dy + t^2 (1 - 2\Gamma_L) dy^2 \right) + b^2 (1 - 2\Psi_L) d\bar{x}^2, \quad (7)$$

with $\Gamma_L = \Phi_L - \Psi_L$ being imposed by the five-dimensional traceless G_j^i equation. The Israel matching conditions at $y = \pm y_0$ then read

$$\Psi_{L,y} = \Gamma_L \frac{nt}{L}, \quad \Phi_{L,y} = -\Gamma_L \frac{nt}{L}, \quad W_L = 0. \quad (8)$$

Performing a series expansion, we find

$$\begin{aligned} \Phi_L = & -\frac{B}{t^2} + \frac{B \operatorname{sech} y_0 \sinh y}{t} + \left(A - \frac{B}{8} - \frac{Bk^2}{4} + \frac{1}{6} Bk^2 \ln |kt| \right. \\ & \left. + \frac{1}{16} B \cosh 2y (-1 + 6 y_0 \coth 2y_0) \operatorname{sech}^2 y_0 - \frac{3}{8} B \operatorname{sech}^2 y_0 \sinh 2y \right) + O(t) \end{aligned} \quad (9)$$

$$\Psi_L = -\frac{B \operatorname{sech} y_0 \sinh y}{t} + \left(2A - \frac{B}{4} + \frac{1}{3} Bk^2 \ln |kt| + \frac{1}{4} B \cosh 2y \operatorname{sech}^2 y_0 \right) + O(t) \quad (10)$$

$$W_L = -\frac{3}{4} B \operatorname{sech}^2 y_0 (y \cosh 2y - y_0 \cosh 2y_0 \sinh 2y) t + O(t^2), \quad (11)$$

where we have set $L = 1$ (to restore L , simply replace $t \rightarrow t/L$ and $k \rightarrow kL$). Except for a few specific instances, we will now adopt this convention throughout the rest of this paper. The two arbitrary constants A and B (which may themselves be arbitrary functions of \vec{k}) have been chosen so that, on the positive-tension brane, to leading order in y_0 , Φ_L goes as

$$\Phi_L = A - \frac{B}{t^2} + O(y_0) + O(k^2) + O(t). \quad (12)$$

IV. EXPANSION IN DIRICHLET/NEUMANN POLYNOMIALS

A. Background

Having solved the relevant five-dimensional Einstein equations as a series expansion in the time t before or after the collision event, we now have an accurate description of the behavior of the bulk at small t for arbitrary collision rapidities. However, in order to match onto the incoming and outgoing states, we really want to study the long-time behavior of the solutions, as the branes become widely separated. Ultimately this will enable us to successfully map the system onto an appropriate four-dimensional effective description. Instead of expanding in powers of the time, we approximate the five-dimensional solution as a power series in the rapidity of the collision, and determine each metric coefficient for all time at each order in the rapidity.

Our main idea is to express the metric as a series of Dirichlet or Neumann polynomials in y_0 and y , bounded at order n by a constant times y_0^n , such that the series satisfies the Israel matching conditions exactly at every order in y_0 . To implement this, we first change variables from b and n to those obeying Neumann boundary conditions. From (4), b/n is Neumann. Likewise, if we define $N(t, y)$ by

$$nt = \frac{1}{N(t, y) - y}, \quad (13)$$

then one can easily check that $N(t, y)$ is also Neumann on the branes. Notice that if N and b/n are constant, the metric (1) is just that for anti-de Sitter spacetime. For fixed y_0 , N describes the proper separation of the two branes, and b is an additional modulus describing the three-dimensional scale-factor of the branes.

Since N and b/n obey Neumann boundary conditions on the branes, we can expand both

in a power series

$$N = N_0(t) + \sum_{n=3}^{\infty} N_n(t) P_n(y), \quad b/n = q_0(t) + \sum_{n=3}^{\infty} q_n(t) P_n(y), \quad (14)$$

where $P_n(y)$ are polynomials

$$P_n(y) = y^n - \frac{n}{n-2} y^{n-2} y_0^2, \quad n = 3, 4, \dots \quad (15)$$

satisfying Neumann boundary conditions and each bounded by $|P_n(y)| < 2y_0^n/(n-2)$, for the relevant range of y . Note that the time-dependent coefficients in this ansatz may also be expanded as a power series in y_0 . By construction, our ansatz satisfies the Israel matching conditions exactly at each order in the expansion. The bulk Einstein equations are not satisfied exactly, but as the expansion is continued, the error terms are bounded by increasing powers of y_0 .

Substituting the series ansätze (14) into the background Einstein equations (2) and (3), we may determine the solution order by order in the rapidity y_0 . At each order in y_0 , one generically obtains a number of linearly independent algebraic equations, and at most one ordinary differential equation in t . The solution of the latter introduces a number of arbitrary constants of integration into the solution.

To fix the arbitrary constants, one first applies the remaining Einstein equations, allowing a small number to be eliminated. The rest are then determined using the series expansion in t presented in the previous section: as this solution is exact to all orders in y_0 , we need only to expand it out to the relevant order in y_0 , before comparing it term by term with our Dirichlet/Neumann polynomial expansion (which is exact in t but perturbative in y_0), taken to a corresponding order in t . The arbitrary constants are then chosen so as to ensure the equivalence of the two expansions in the region where both t and y_0 are small. This procedure suffices to fix all the remaining arbitrary constants.

The first few terms of the solution are

$$N_0 = \frac{1}{t} - \frac{1}{2} t y_0^2 + \frac{1}{24} t (8 - 9t^2) y_0^4 + \dots \quad (16)$$

$$N_3 = -\frac{1}{6} + \left(\frac{5}{72} - 2t^2 \right) y_0^2 + \dots \quad (17)$$

and

$$q_0 = 1 - \frac{3}{2} t^2 y_0^2 + \left(t^2 - \frac{7}{8} t^4 \right) y_0^4 + \dots \quad (18)$$

$$q_3 = -2 t^3 y_0^2 + \dots, \quad (19)$$

and the full solution up to $O(y_0^{10})$ may be found in Appendix B.

B. Perturbations

Following the same principles used in our treatment of the background, we construct the two linear combinations

$$\phi_4 = \frac{1}{2}(\Phi_L + \Psi_L), \quad \xi_4 = b^2(\Psi_L - \Phi_L) = b^2\Gamma_L, \quad (20)$$

both of which obey Neumann boundary conditions on the branes, as may be checked from (4) and (8). In addition, W_L already obeys simple Dirichlet boundary conditions.

The two Neumann variables, ϕ_4 and ξ_4 , are then expanded in a series of Neumann polynomials and W_L is expanded in a series of Dirichlet polynomials,

$$D_n(y) = y^n - y_0^n, \quad n = 2, 4, \dots, \quad D_n(y) = y D_{n-1}(y), \quad n = 3, 5, \dots, \quad (21)$$

each bounded by $|D_n(y)| < y_0^n$ for n even and $y_0^n(n-1)/n^{n/(n-1)}$ for n odd, over the relevant range of y . As in the case of the background, the time-dependent coefficients multiplying each of the polynomials should themselves be expanded in powers of y_0 .

To solve for the perturbations it is sufficient to use only three of the perturbed Einstein equations (any solution obtained may then be verified against the remainder). Setting

$$\Phi_L = \phi e^{-2\nu-\beta/3} \quad (22)$$

$$\Psi_L = \psi e^{-\beta/3} \quad (23)$$

$$W_L = w e^{\tau-2\nu-\beta/3} \quad (24)$$

where $t = e^\tau$, $\beta = 3 \ln b$ and $\nu = \ln nt$, the G_i^5 , G_i^0 and G_i^i equations take the form

$$w_{,\tau} = 2\phi_{,y} - 4e^{3\nu/2}(\psi e^{\nu/2})_{,y} \quad (25)$$

$$\phi_{,\tau} = \frac{1}{2}w_{,y} - e^{3\nu}(\psi e^{-\nu})_{,\tau} \quad (26)$$

$$\begin{aligned} (\psi_{,\tau} e^{\beta/3})_{,\tau} &= (\psi_{,y} e^{\beta/3})_{,y} + \psi e^{\beta/3} \left(\frac{1}{3} \beta_{,\tau}^2 - \frac{1}{9} \beta_{,y}^2 - k^2 e^{2(\nu-\beta/3)} \right) \\ &\quad - \frac{2}{9} e^{-2\nu+\beta/3} (\phi(\beta_{,\tau}^2 + \beta_{,y}^2) - w \beta_{,\tau} \beta_{,y}). \end{aligned} \quad (27)$$

Using our Neumann and Dirichlet ansätze for ϕ_4 , ξ_4 and W_L , the Israel matching conditions are automatically satisfied and it remains only to solve (25), (26) and (27) order by

order in the rapidity. The time-dependent coefficients for ϕ_4 , ξ_4 and W_L are then found to obey simple ordinary differential equations, with solutions comprising Bessel functions in kt , given in Appendix C. Note that it is not necessary for the set of Neumann or Dirichlet polynomials we have used to be orthogonal to each other: linear independence is perfectly sufficient to determine all the time-dependent coefficients order by order in y_0 .

As in the case of the background, the arbitrary constants of integration remaining in the solution after the application of the remaining Einstein equations are fixed by performing a series expansion of the solution in t . This expansion can be compared term by term with the series expansion in t given previously, after this latter series has itself been expanded in y_0 . The arbitrary constants are then chosen so that the two expansions coincide in the region where both t and y_0 are small. The results of these calculations, at long wavelengths, are:

$$\Phi_L = A - B \left(\frac{1}{t^2} - \frac{k^2}{6} \ln|kt| \right) + \left(At + \frac{B}{t} \right) y + \dots \quad (28)$$

$$\Psi_L = 2A + B \frac{k^2}{3} \ln|kt| - \left(At + \frac{B}{t} \right) y + \dots \quad (29)$$

$$W_L = 6A t^2 (y^2 - y_0^2) + \dots \quad (30)$$

where the constants A and B can be arbitrary functions of k . The solutions for all k , to fifth order in y_0 , are given in Appendix C.

V. EXPANSION ABOUT THE SCALING SOLUTION

It is illuminating to recast the results of the preceding sections in terms of a set of dimensionless variables. Using the relative velocity of the branes at the moment of collision, $V = 2c \tanh y_0 \simeq 2cy_0$ (where we have temporarily re-introduced the speed of light c), we may construct the dimensionless time parameter $x = y_0 ct/L \sim Vt/L$ and the dimensionless y -coordinate $\omega = y/y_0 \sim y(c/V)$.

Starting from the full Dirichlet/Neumann polynomial expansion for the background given in Appendix B, restoring c to unity and setting $t = xL/y_0$ and $y = \omega y_0$, we find that

$$n^{-1} = \tilde{N}(x) - \omega x + O(y_0^2) \quad (31)$$

$$\frac{b}{n} = q(x) + O(y_0^2), \quad (32)$$

where

$$\tilde{N}(x) = 1 - \frac{x^2}{2} - \frac{3x^4}{8} - \frac{25x^6}{48} - \frac{343x^8}{384} - \frac{2187x^{10}}{1280} + O(x^{12}) \quad (33)$$

$$q(x) = 1 - \frac{3x^2}{2} - \frac{7x^4}{8} - \frac{55x^6}{48} - \frac{245x^8}{128} - \frac{4617x^{10}}{1280} + O(x^{12}). \quad (34)$$

The single term in (31) linear in ω is necessary in order that n^{-1} satisfies the correct boundary conditions. Apart from this one term, however, we see that to lowest order in y_0 the metric functions above turn out to be completely independent of ω . Similar results are additionally found for the perturbations.

Later, we will see how this behavior leads to the emergence of a four-dimensional effective theory. For now, the key point to notice is that this series expansion converges only for $x \ll 1$, corresponding to times $t \ll L/y_0$. In order to study the behavior of the theory for all times therefore, we require a means of effectively resumming the above perturbation expansion to all orders in x . Remarkably, we will be able to accomplish just this. The remainder of this section, divided into five parts, details our method and results: first, we explain how to find and expand about the scaling solution, considering only the background for simplicity. We then analyze various aspects of the background scaling solution, namely, the brane geometry and the analytic continuation required to go to late times, before moving on to discuss higher-order terms in the expansion. Finally, we extend our treatment to cover the perturbations.

A. Scaling solution for the background

The key to the our method is the observation that the approximation of small collision rapidity ($y_0 \ll 1$) leads to a set of equations that are perturbatively ultralocal: transforming to the dimensionless coordinates x and ω , the Einstein equations for the background (2) and (3) become

$$\beta_{,\omega\omega} + \beta_{,\omega}^2 - 12e^{2\tilde{\nu}} = y_0^2 (x(x\beta_{,x}),_x + x^2\beta_{,x}^2) \quad (35)$$

$$\tilde{\nu}_{,\omega\omega} - \frac{1}{3}\beta_{,\omega}^2 + 2e^{2\tilde{\nu}} = y_0^2 (x(x\tilde{\nu}_{,x}),_x - \frac{1}{3}x^2\beta_{,x}^2), \quad (36)$$

where we have introduced $\tilde{\nu} = \nu + \ln y_0$. Strikingly, all the terms involving x -derivatives are now suppressed by a factor of y_0^2 relative to the remaining terms. This segregation of x - and ω -derivatives has profound consequences: when solving perturbatively in y_0 , the Einstein

equations (35) and (36) reduce to a series of *ordinary* differential equations in ω , as opposed to the partial differential equations we started off with.

To see this, consider expanding out both the Einstein equations (35) and (36) as well as the metric functions β and $\tilde{\nu}$ as a series in positive powers of y_0 . At zeroth order in y_0 , the right-hand sides of (35) and (36) vanish, and the left-hand sides can be integrated with respect to ω to yield anti-de Sitter space. (This was our reason for using $\tilde{\nu} = \nu + \ln y_0$ rather than ν : the former serves to pull the necessary exponential term deriving from the cosmological constant down to zeroth order in y_0 , yielding anti-de Sitter space as a solution at leading order. As we are merely adding a constant, the derivatives of $\tilde{\nu}$ and ν are identical.) The Israel matching conditions on the branes (4), which in these coordinates read

$$\frac{1}{3} \beta_{,\omega} = \tilde{\nu}_{,\omega} = e^{\tilde{\nu}}, \quad (37)$$

are not however sufficient to fix all the arbitrary functions of x arising in the integration with respect to ω . In fact, two arbitrary functions of x remain in the solution, which may be regarded as time-dependent moduli describing the three-dimensional scale factor of the branes and their proper separation. These moduli may be determined with the help of the G_5^5 Einstein equation as we will demonstrate shortly.

Returning to (35) and (36) at y_0^2 order now, the left-hand sides amount to ordinary differential equations in ω for the y_0^2 corrections to β and $\tilde{\nu}$. The right-hand sides can no longer be neglected, but, because of the overall factor of y_0^2 , only the time-derivatives of β and $\tilde{\nu}$ at zeroth order in y_0 are involved. Since β and $\tilde{\nu}$ have already been determined to this order, the right-hand sides therefore act merely as known source terms. Solving these ordinary differential equations then introduces two further arbitrary functions of x ; these serve as y_0^2 corrections to the time-dependent moduli and may be fixed in the same manner as previously.

Our integration scheme therefore proceeds at each order in y_0 via a two-step process: first, we integrate the Einstein equations (35) and (36) to determine the ω -dependence of the bulk geometry, and then secondly, we fix the x -dependent moduli pertaining to the brane geometry using the G_5^5 equation. This latter step works as follows: evaluating the G_5^5 equation on the branes, we can use the Israel matching conditions (37) to replace the single ω -derivatives that appear in this equation, yielding an ordinary differential equation in time

for the geometry on each brane. Explicitly, we find

$$\left(\frac{bb_{,x}}{n} \right)_{,x} = 0, \quad (38)$$

where five-dimensional considerations (see Section VI) further allow us to fix the constants of integration on the (\pm) brane as

$$\frac{bb_{,x}}{n} = \frac{bb_{,t}}{y_0 n} = \frac{b_{,t\pm}}{y_0} = \pm \frac{1}{y_0} \tanh y_0, \quad (39)$$

where the brane conformal time t_\pm is defined on the branes via $ndt = bdt_\pm$. When augmented with the initial conditions that n and b both tend to unity as x tends to zero (so that we recover compactified Milne spacetime near the collision), these two equations are fully sufficient to determine the two x -dependent moduli to all orders in y_0 .

Putting the above into practice, for convenience we will work with the Neumann variables \tilde{N} and q , generalizing (31) and (32) to

$$n^{-1} = \tilde{N}(x, \omega) - \omega x, \quad \frac{b}{n} = q(x, \omega). \quad (40)$$

Seeking an expansion of the form

$$\tilde{N}(x, \omega) = \tilde{N}_0(x, \omega) + y_0^2 \tilde{N}_1(x, \omega) + O(y_0^4) \quad (41)$$

$$q(x, \omega) = q_0(x, \omega) + y_0^2 q_1(x, \omega) + O(y_0^4), \quad (42)$$

the Einstein equations (35) and (36) when expanded to zeroth order in y_0 immediately restrict \tilde{N}_0 and q_0 to be functions of x alone. The bulk geometry to this order is then simply anti-de Sitter space with time-varying moduli, consistent with (31) and (32). The moduli $\tilde{N}_0(x)$ and $q_0(x)$ may be found by integrating the brane equations (39), also expanded to lowest order in y_0 . In terms of the Lambert W-function [31], $W(x)$, defined implicitly by

$$W(x)e^{W(x)} = x, \quad (43)$$

the solution is

$$\tilde{N}_0(x) = e^{\frac{1}{2}W(-x^2)}, \quad q_0(x) = (1 + W(-x^2)) e^{\frac{1}{2}W(-x^2)}. \quad (44)$$

Thus we have found the scaling solution for the background, whose form is independent of y_0 , holding for any $y_0 \ll 1$. Using the series expansion for the Lambert W-function about $x = W(x) = 0$, namely [32]

$$W(x) = \sum_{m=1}^{\infty} \frac{(-m)^{m-1}}{m!} x^m, \quad (45)$$

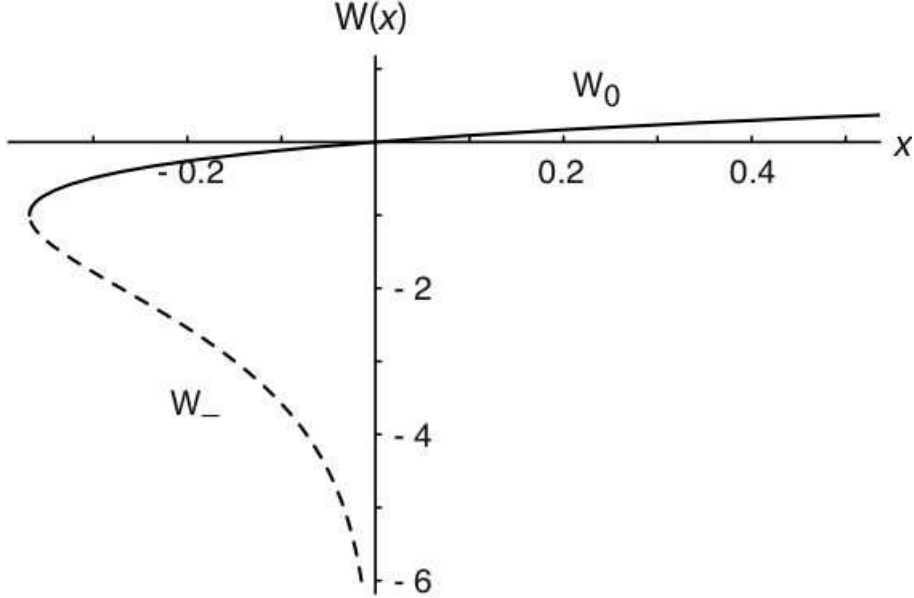


Figure 2: The real values of the Lambert W-function. The solid line indicates the principal solution branch, $W_0(x)$, while the dashed line depicts the $W_{-1}(x)$ branch. The two branches join smoothly at $x = -1/e$ where W attains its negative maximum of -1 .

we can immediately check that the expansion of our solution is in exact agreement with (33) and (34). At leading order in y_0 then, we have succeeded in resumming the Dirichlet/Neumann polynomial expansion results for the background to all orders in x .

Later, we will return to evaluate the y_0^2 corrections in our expansion about the scaling solution. In the next two subsections, however, we will first examine the scaling solution in greater detail.

B. Evolution of the brane scale factors

Using the scaling solution (44) to evaluate the scale factors on both branes, we find to $O(y_0^2)$

$$b_{\pm} = 1 \pm x e^{-\frac{1}{2}W(-x^2)} = 1 \pm \sqrt{-W(-x^2)}. \quad (46)$$

To follow the evolution of the brane scale factors, it is helpful to first understand the behavior of the Lambert W-function, the real values of which are displayed in Figure 2. For positive arguments the Lambert W-function is single-valued, however, for the negative arguments of interest here, we see that there are in fact two different real solution branches. The first

branch, denoted $W_0(x)$, satisfies $W_0(x) \geq -1$ and is usually referred to as the principal branch, while the second branch, $W_{-1}(x)$, is defined in the range $W_{-1}(x) \leq -1$. The two solution branches join smoothly at $x = -1/e$, where $W = -1$.

Starting at the brane collision where $x = 0$, the brane scale factors are chosen to satisfy $b_{\pm} = 1$, and so we must begin on the principal branch of the Lambert W-function for which $W_0(0) = 0$. Thereafter, as illustrated in Figure 3, b_+ increases and b_- decreases monotonically until at the critical time $x = x_c$, when $W_0(-x_c^2) = -1$ and b_- shrinks to zero. From (43), the critical time is therefore $x_c = e^{-\frac{1}{2}} = 0.606\dots$, and corresponds physically to the time at which the negative-tension brane encounters the bulk black hole [33].

At this moment, the scale factor on the positive-tension brane has only attained a value of two. From the Birkhoff-frame solution, in which the bulk is Schwarzschild-AdS and the branes are moving, we know that the positive-tension brane is unaffected by the disappearance of the negative-tension brane and simply continues its journey out to the boundary of AdS. To reconcile this behavior with our solution in brane-static coordinates, it is helpful to pass to t_+ , the conformal time on the positive-tension brane. Working to zeroth order in y_0 , this may be converted into the dimensionless form

$$x_4 = \frac{y_0 t_+}{L} = \frac{y_0}{L} \int \frac{n}{b} dt = \int \frac{dx}{q_0(x)} = x e^{-\frac{1}{2}W(-x^2)} = \sqrt{-W(-x^2)}. \quad (47)$$

Inverting this expression, we find that the bulk time parameter $x = x_4 e^{-\frac{1}{2}x_4^2}$. The bulk time x is thus double-valued when expressed as a function of x_4 , the conformal time on the positive-tension brane: to continue forward in x_4 beyond $x_4 = 1$ (where $x = x_c$), the bulk time x must reverse direction and decrease towards zero. The metric functions, expressed in terms of x , must then continue back along the other branch of the Lambert W-function, namely the W_{-1} branch. In this manner we see that the solution for the scale factor on the positive-tension brane, when continued on to the W_{-1} branch, tends to infinity as the bulk time x is reduced back towards zero (see dotted line in Figure 3), corresponding to the positive-tension brane approaching the boundary of AdS as $x_4 \rightarrow \infty$.

For simplicity, in the remainder of this paper we will work directly with the brane conformal time x_4 itself. With this choice, the brane scale factors to zeroth order in y_0 are simply $b_{\pm} = 1 \pm x_4$.

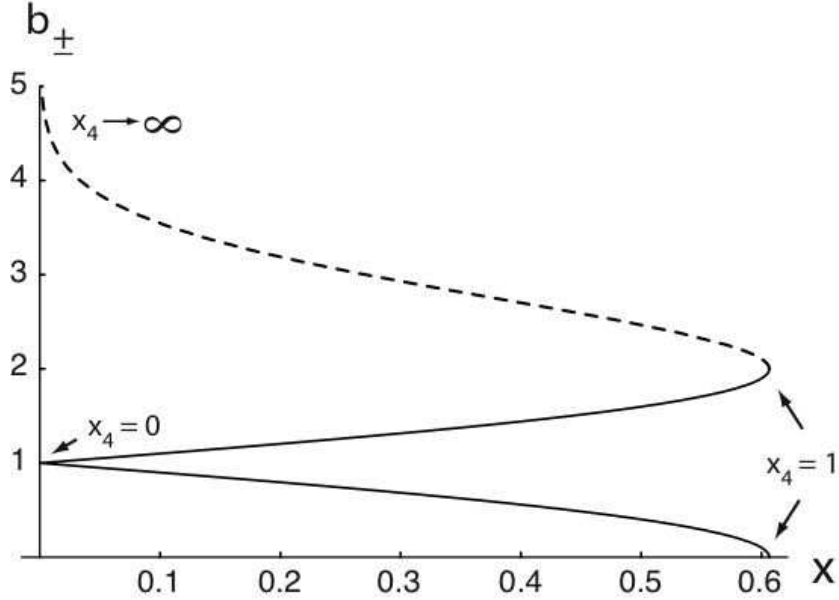


Figure 3: The scale factors b_{\pm} on the positive-tension brane (rising curve) and negative-tension brane (falling curve) as a function of the bulk time parameter x , to zeroth order in y_0 . The continuation of the positive-tension brane scale factor on to the W_{-1} branch of the Lambert W-function is indicated by the dashed line.

C. Analytic continuation of the bulk geometry

In terms of x_4 , the metric functions n and b are given by

$$n = \frac{e^{\frac{1}{2}x_4^2}}{1 - \omega x_4} + O(y_0^2), \quad b = \frac{1 - x_4^2}{1 - \omega x_4} + O(y_0^2). \quad (48)$$

At $x_4 = 1$, the three-dimensional scale factor b shrinks to zero at all values of ω except $\omega = 1$ (*i.e.* the positive-tension brane). Since b is a coordinate scalar under transformations of x_4 and ω , one might be concerned that the scaling solution becomes singular at this point. However, when we compute the y_0^2 corrections as we will do shortly, we will find that the corrections become large close to $x_4 = 1$, precipitating a breakdown of the small- y_0 expansion. Since it will later turn out that the scaling solution maps directly on to the four-dimensional effective theory, and that this, like the metric on the positive-tension brane, is completely regular at $x_4 = 1$, we are encouraged to simply analytically continue the scaling solution to times $x_4 > 1$.

When implementing this analytic continuation careful attention must be paid to the range of the coordinate ω . Thus far, for times $x_4 < 1$, we have regarded ω as a coordinate

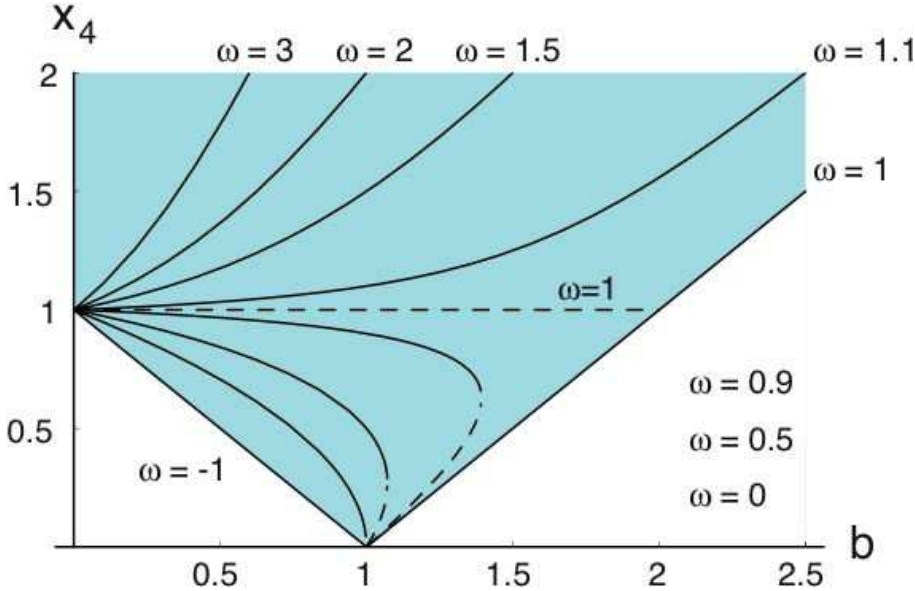


Figure 4: The contours of constant ω in the (b, x_4) plane. Working to zeroth order in y_0 , these are given by $x_4 = \frac{1}{2}(b\omega \pm \sqrt{b^2\omega^2 - 4(b-1)})$, where we have plotted the positive root using a solid line and the negative root using a dashed line. The negative-tension brane is located at $\omega = -1$ for times $x_4 < 1$, and the trajectory of the positive-tension brane is given (for all time) by the positive root solution for $\omega = 1$. The region delimited by the trajectories of the branes (shaded) then corresponds to the bulk. From the plot we see that, for $0 < x_4 < 1$, the bulk is parameterized by values of ω in the range $-1 \leq \omega \leq 1$. In contrast, for $x_4 > 1$, the bulk is parameterized by values of ω in the range $\omega \geq 1$.

spanning the fifth dimension, taking values in the range $-1 \leq \omega \leq 1$. The two metric functions n and b were then expressed in terms of the coordinates x_4 and ω . Strictly speaking, however, this parameterization is redundant: we could have chosen to eliminate ω by promoting the three-dimensional scale factor b from a metric function to an independent coordinate parameterizing the fifth dimension. Thus we would have only one metric function n , expressed in terms of the coordinates x_4 and b .

While this latter parameterization is more succinct, its disadvantage is that the locations of the branes are no longer explicit, since the value of the scale factor b on the branes is time-dependent. In fact, to track the location of the branes we must re-introduce the function $\omega(x_4, b) = (b + x_4^2 - 1)/bx_4$ (inverting (48) at lowest order in y_0). The trajectories of the branes are then given by the contours $\omega = \pm 1$.

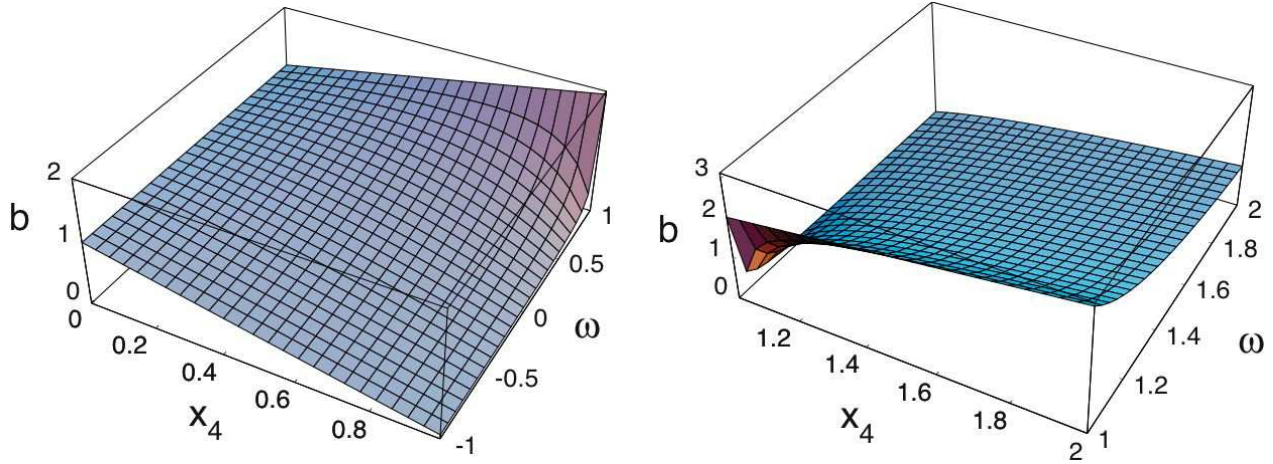


Figure 5: The three-dimensional scale factor b , plotted to zeroth order in y_0 as a function of x_4 and ω , for $x_4 < 1$ (left) and $x_4 > 1$ (right). The positive-tension brane is fixed at $\omega = 1$ for all time (note the evolution of its scale factor is smooth and continuous), and for $x_4 < 1$, the negative-tension brane is located at $\omega = -1$.

The contours of constant ω as a function of x_4 and b are plotted in Figure 4. The analytic continuation to times $x_4 > 1$ has been implemented, and the extent of the bulk is indicated by the shaded region. From the figure, we see that, if we were to revert to our original parameterization of the bulk in terms of x_4 and ω , the range of ω required depends on the time coordinate x_4 : for early times $x_4 < 1$, we require only values of ω in the range $-1 \leq \omega \leq 1$, whereas for late times $x_4 > 1$, we require values in the range $\omega \geq 1$. Thus, while the positive-tension brane remains fixed at $\omega = 1$ throughout, at early times $x_4 < 1$ the value of ω *decreases* as we head away from the positive-tension brane along the fifth dimension, whereas at late times $x_4 > 1$, the value of ω *increases* away from the positive-tension brane.

While this behavior initially appears paradoxical if ω is regarded as a coordinate along the fifth dimension, we stress that the only variables with meaningful physical content are the brane conformal time x_4 and the three-dimensional scale factor b . These physical variables behave sensibly under analytic continuation. In contrast, ω is simply a convenient parameterization introduced to follow the brane trajectories, with the awkward feature that its range alters under the analytic continuation at $x_4 = 1$.

For the rest of this paper, we will find it easiest to continue parameterizing the bulk in terms of x_4 and ω , adjusting the range of the ω where required. Figure 5 illustrates this approach: at early times $x_4 < 1$ the three-dimensional scale factor b is plotted for values of

ω in the range $-1 \leq \omega \leq 1$. At late times $x_4 > 1$, we must however plot b for values of ω in the range $\omega \geq 1$. In this fashion, the three-dimensional scale factor b always decreases along the fifth dimension away from the brane.

We have argued that the scaling solution for the background, obtained at lowest order in y_0 , may be analytically continued across $x_4 = 1$. There is a coordinate singularity in the x_4, ω coordinates but this does not affect the metric on the positive-tension brane which remains regular throughout. The same features will be true when we solve for the cosmological perturbations. The fact that the continuation is regular on the positive-tension brane and precisely agrees with the predictions of the four-dimensional effective theory provides strong evidence for its correctness. Once the form of the the background and the perturbations have been determined to lowest order in y_0 , the higher-order corrections are obtained from differential equations in y with source terms depending only on the lowest order solutions. It is straightforward to obtain these corrections for $x_4 < 1$. If we analytically continue them as described to $x_4 > 1$ as described, we automatically solve the bulk Einstein equations and the Israel matching conditions on the positive tension brane for all x_4 . The continued solution is well-behaved after the collision in the vicinity of the positive-tension brane, out to large distances where the y_0 expansion fails.

D. Higher-order corrections

In this section we explicitly compute the y_0^2 corrections. The size of these corrections indicates the validity of the expansion about the scaling solution, which perforce is only valid when the y_0^2 corrections are small.

Following the procedure outlined previously, we first evaluate the Einstein equations (35) and (36) to $O(y_0^2)$ using the ansätze (41) and (42), along with the solutions for $\tilde{N}_0(x)$ and $q_0(x)$ given in (44). The result is two second-order ordinary differential equations in ω , which may straightforwardly be integrated yielding $\tilde{N}_1(x, \omega)$ and $q_1(x, \omega)$ up to two arbitrary functions of x_4 . These time-dependent moduli are then fixed using the brane equations (39), evaluated at $O(y_0^2)$ higher than previously.

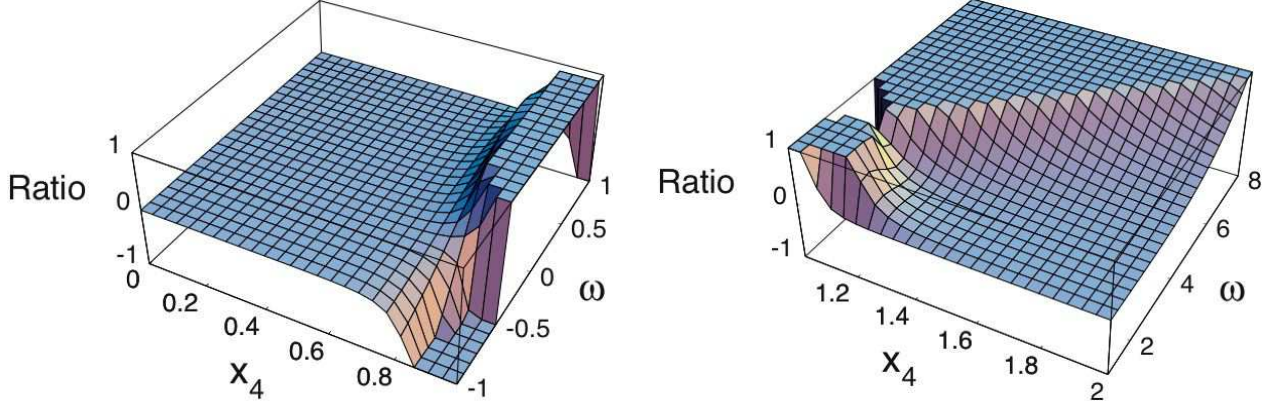


Figure 6: The ratio of the y_0^2 corrections to the leading term in the small- y_0 expansion for b , plotted for $x_4 < 1$ (left) and $x_4 > 1$ (right), for the case where $y_0 = 0.1$. Where this ratio becomes of order unity the expansion about the scaling solution breaks down. The analogous plots for n display similar behavior.

We obtain the result:

$$n(x_4, \omega) = \frac{e^{\frac{1}{2}x_4^2}}{1 - \omega x_4} + \frac{e^{\frac{1}{2}x_4^2} y_0^2}{30(-1 + \omega x_4)^2 (-1 + x_4^2)^4} \left(x_4 (5\omega(-3 + \omega^2) - 5x_4 + 40\omega(-3 + \omega^2)x_4^2 - 5(-14 + 9\omega^2(-2 + \omega^2))x_4^3 + 3\omega^3(-5 + 3\omega^2)x_4^4 - 19x_4^5 + 5x_4^7) - 5(-1 + x_4^2)^3 \ln(1 - x_4^2) \right) + O(y_0^4), \quad (49)$$

$$b(x_4, \omega) = \frac{1 - x_4^2}{1 - \omega x_4} + \frac{x_4 y_0^2}{30(-1 + \omega x_4)^2 (-1 + x_4^2)^3} \left(-5\omega(-3 + \omega^2) - 20x_4 + 5\omega(-7 + 4\omega^2)x_4^2 - 10(1 - 12\omega^2 + 3\omega^4)x_4^3 + 3\omega(-20 - 5\omega^2 + 2\omega^4)x_4^4 - 12x_4^5 + 31\omega x_4^6 - 5\omega x_4^8 - 5(-1 + x_4^2)^2(\omega - 2x_4 + \omega x_4^2) \ln(1 - x_4^2) \right) + O(y_0^4). \quad (50)$$

In Figure 6, we have plotted the ratio of the y_0^2 corrections to the corresponding terms at leading order: where this ratio becomes of order unity the expansion about the scaling solution breaks down. Inspection shows there are two such regions: the first is for times close to $x_4 = 1$, for all ω , and the second occurs at late times $x_4 > 1$, far away from the positive-tension brane. In neither case does the failure of the y_0 expansion indicate a singularity of the background metric: from the bulk-static coordinate system we know the exact solution for the background metric is simply Schwarzschild-AdS, which is regular everywhere. The exact bulk-static solution in Birkhoff frame tells us that the proper speed of the negative-

tension brane, relative to the static bulk, approaches the speed of light as it reaches the event horizon of the bulk black hole. It therefore seems plausible that a small- y_0 expansion based upon slowly-moving branes must break down at this moment, when $x_4 = 1$ in our chosen coordinate system.

Analytically continuing our solution in both x_4 and ω around $x_4 = 1$, the logarithmic terms in the y_0^2 corrections now acquire imaginary pieces for $x_4 > 1$. However, since these imaginary terms are all suppressed by a factor of y_0^2 , they can only enter the Einstein-brane equations (expanded as a series to y_0^2 order) in a linear fashion. Hence the real and imaginary parts of the metric necessarily constitute *independent* solutions, permitting us to simply throw away the imaginary part and work with the real part alone. As a confirmation of this, it can be checked explicitly that replacing the $\ln(1 - x_4)$ terms in (49) and (50) with $\ln|1 - x_4|$ still provides a valid solution to $O(y_0^2)$ of the complete Einstein-brane equations and boundary conditions.

Finally, at late times where $x_4 > 1$, note that the extent to which we know the bulk geometry away from the positive-tension brane is limited by the y_0^2 corrections, which become large at an increasingly large value of ω , away from the positive-tension brane (see Figure 6). The expansion about the scaling solution thus breaks down before we reach the horizon of the bulk black hole, which is located at $\omega \rightarrow \infty$ for $x_4 > 1$.

E. Treatment of the perturbations

Having determined the background geometry to $O(y_0^2)$ in the preceding subsections, we now turn our attention to the perturbations. In this subsection we show how to evaluate the perturbations to $O(y_0^2)$ by expanding about the scaling solution. The results will enable us to perform stringent checks of the four-dimensional effective theory and moreover to evaluate the mode-mixing between early and late times.

In addition to the dimensionless variables $x = y_0 ct/L$ and $\omega = y/y_0$, when we consider the metric perturbations we must further introduce the dimensionless perturbation amplitude $\tilde{B} = B y_0^2 c^2 / L^2 \sim B V^2 / L^2$ and the dimensionless wavevector $\tilde{k} = k L / y_0 \sim c k L / V$. In this fashion, to lowest order in y_0 and k , we then find $\Phi_L = A - B/t^2 = A - \tilde{B}/x^2$ and similarly $kct = \tilde{k}x$. (Note that the perturbation amplitude A is already dimensionless however).

Following the treatment of the perturbations in the Dirichlet/Neumann polynomial ex-

pansion, we will again express the metric perturbations in terms of W_L (obeying Dirichlet boundary conditions), and the Neumann variables ϕ_4 and ξ_4 , defined in (20). Hence we seek an expansion of the form

$$\phi_4(x_4, \omega) = \phi_{40}(x_4, \omega) + y_0^2 \phi_{41}(x_4, \omega) + O(y_0^4), \quad (51)$$

$$\xi_4(x_4, \omega) = \xi_{40}(x_4, \omega) + y_0^2 \xi_{41}(x_4, \omega) + O(y_0^4), \quad (52)$$

$$W_L(x_4, \omega) = W_{L0}(x_4, \omega) + y_0^2 W_{L1}(x_4, \omega) + O(y_0^4). \quad (53)$$

As in the case of the background, we will use the G_5^5 equation evaluated on the brane to fix the arbitrary functions of x_4 arising from integration of the Einstein equations with respect to ω . By substituting the Israel matching conditions into the G_5^5 equation, along with the boundary conditions for the perturbations, it is possible to remove the single ω -derivatives that appear. We arrive at the following second-order ordinary differential equation, valid on both branes,

$$\begin{aligned} 0 = & 2n(x_4^2 - 1)(2b^2\phi_4 + \xi_4)\dot{b}^2 + b^2 \left(nx_4(x_4^2 - 3) - (x_4^2 - 1)\dot{n} \right) (2b^2\dot{\phi}_4 - \dot{\xi}_4) \\ & + b\dot{b} \left(4nx_4(x_4^2 - 3)(b^2\phi_4 + \xi_4) - (x_4^2 - 1)(4(b^2\phi_4 + \xi_4)\dot{n} - n(10b^2\dot{\phi}_4 + \dot{\xi}_4)) \right) \\ & + bn(x_4^2 - 1) \left(4(b^2\phi_4 + \xi_4)\ddot{b} + 2b^3\ddot{\phi}_4 - b\ddot{\xi}_4 \right), \end{aligned} \quad (54)$$

where dots indicate differentiation with respect to x_4 , and where, in the interests of brevity, we have omitted terms of $O(\tilde{k}^2)$.

Beginning our computation, the G_i^5 and G_5^5 Einstein equations when evaluated to lowest order in y_0 immediately restrict ϕ_{40} and ξ_{40} to be functions of x_4 only. Integrating the G_i^0 equation with respect to ω then gives W_{L0} in terms of ϕ_{40} and ξ_{40} , up to an arbitrary function of x_4 . Requiring that W_{L0} vanishes on both branes allows us to both fix this arbitrary function, and also to solve for ξ_{40} in terms of ϕ_{40} alone. Finally, evaluating (54) on both branes to lowest order in y_0 and solving simultaneously yields a second-order ordinary differential equation for ϕ_{40} , with solution

$$\phi_{40} = \left(\frac{3A}{2} - \frac{9\tilde{B}}{16} \right) - \frac{\tilde{B}}{2x_4^2} + O(\tilde{k}^2), \quad (55)$$

where the two arbitrary constants have been chosen to match the small- t series expansion

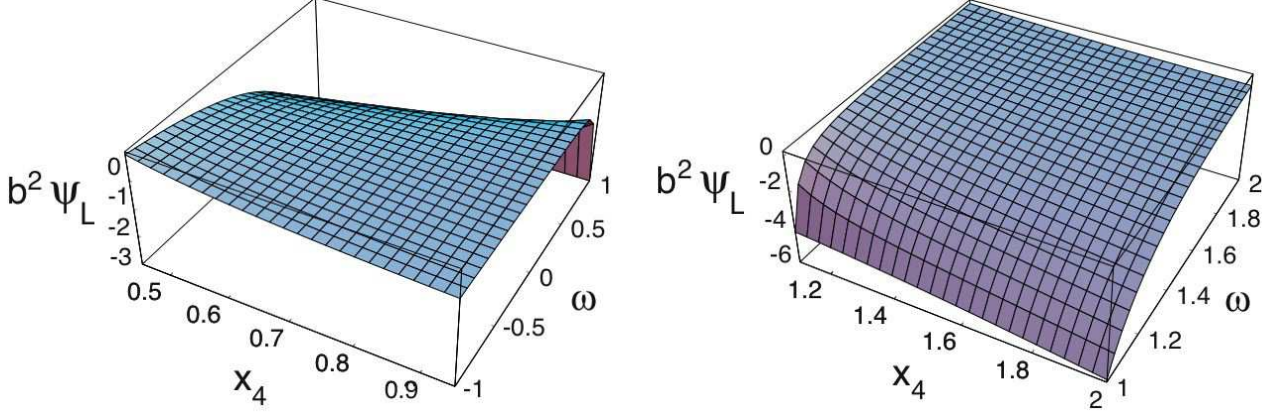


Figure 7: The perturbation to the three-dimensional scale factor, $b^2 \Psi_L$, plotted on long wavelengths to zeroth order in y_0 for early times (left) and late times (right). Only the \tilde{B} mode is displayed (*i.e.* $A = 0$ and $\tilde{B} = 1$). Note how the perturbations are localized on the positive-tension brane (located at $\omega = 1$), and decay away from the brane.

given in Section III. With this choice,

$$\xi_{40} = -A + \frac{11\tilde{B}}{8} - \frac{\tilde{B}}{x_4^2} + \left(A - \frac{3\tilde{B}}{8} \right) x_4^2 + O(\tilde{k}^2) \quad (56)$$

$$W_{L0} = e^{-\frac{1}{2}x_4^2} \frac{(1 - \omega^2)}{(1 - x_4^2)^2} \left(3Ax_4^2(-2 + \omega x_4) + \tilde{B}x_4\left(\frac{9}{4}x_4 + \omega(1 - \frac{9}{8}x_4^2)\right) \right) + O(\tilde{k}^2). \quad (57)$$

The resulting behavior for the perturbation to the three-dimensional scale factor, $b^2 \Psi_L$, is plotted in Figure 7.

In terms of the original Newtonian gauge variables, an identical calculation (working now to all orders in \tilde{k}) yields,

$$\begin{aligned} \Phi_L &= \frac{2\tilde{k}(1 - \omega x_4)^2}{3(x_4^2 - 1)} (A_0 J_0(\tilde{k}x_4) + B_0 Y_0(\tilde{k}x_4)) \\ &\quad + \frac{1}{x_4} \left(1 + \frac{(1 - \omega x_4)^2}{1 - x_4^2} \right) (A_0 J_1(\tilde{k}x_4) + B_0 Y_1(\tilde{k}x_4)) + O(y_0^2), \end{aligned} \quad (58)$$

$$\begin{aligned} \Psi_L &= \frac{1}{3(1 - x_4^2)} \left(2\tilde{k}(1 - \omega x_4)^2 (A_0 J_0(\tilde{k}x_4) + B_0 Y_0(\tilde{k}x_4)) \right. \\ &\quad \left. - 3(x_4 + \omega(-2 + \omega x_4)) (A_0 J_1(\tilde{k}x_4) + B_0 Y_1(\tilde{k}x_4)) \right) + O(y_0^2), \end{aligned} \quad (59)$$

$$\begin{aligned} W_L &= 2x_4^2 e^{-\frac{1}{2}x_4^2} \frac{(\omega^2 - 1)}{(1 - x_4^2)^2} \left(\tilde{k}(1 - \omega x_4) (A_0 J_0(\tilde{k}x_4) + B_0 Y_0(\tilde{k}x_4)) \right. \\ &\quad \left. + \omega (A_0 J_1(\tilde{k}x_4) + B_0 Y_1(\tilde{k}x_4)) \right) + O(y_0^2), \end{aligned} \quad (60)$$

where the constants A_0 and B_0 are given by

$$A_0 = \frac{3A}{\tilde{k}} - \frac{9\tilde{B}}{8\tilde{k}} + \frac{1}{2}\tilde{B}\tilde{k}(\ln 2 - \gamma) + O(y_0^2), \quad B_0 = \frac{\tilde{B}\tilde{k}\pi}{4} + O(y_0^2). \quad (61)$$

To evaluate the y_0^2 corrections, we repeat the same sequence of steps: integrating the G_i^5 and G_5^5 Einstein equations (at y_0^2 higher order) gives us ϕ_{41} and ξ_{41} up to two arbitrary functions of x_4 , and integrating the G_i^0 equation then gives us W_{L1} in terms of these two arbitrary functions plus one more. Two of the three arbitrary functions are then determined by imposing the Dirichlet boundary conditions on W_{L1} , and the third is found to satisfy a second-order ordinary differential equation after making use of (54) on both branes. This can be solved, and the constants of integration appearing in the solution are again chosen so as to match the small- t series expansion of Section III.

Converting back to the original longitudinal gauge variables, the results to $O(y_0^4)$ and to $O(k^2)$ take the schematic form

$$\Phi_L = f_0^\Phi + y_0^2(f_1^\Phi + f_2^\Phi \ln(1+x_4) + f_3^\Phi \ln(1-x_4) + f_4^\Phi \ln(1-\omega x_4)), \quad (62)$$

$$\Psi_L = f_0^\Psi + y_0^2(f_1^\Psi + f_2^\Psi \ln(1+x_4) + f_3^\Psi \ln(1-x_4) + f_4^\Psi \ln(1-\omega x_4)), \quad (63)$$

$$W_L = e^{-\frac{1}{2}x_4^2} (f_0^W + y_0^2(f_1^W + f_2^W \ln(1+x_4) + f_3^W \ln(1-x_4) + f_4^W \ln(1-\omega x_4))), \quad (64)$$

where the f are rational functions of x_4 and ω which, due to their length, have been listed separately in Appendix D. (If desired, more detailed results including the $O(k^2)$ corrections are available [27]).

It is easy to check that the results obtained by expanding about the scaling solution are consistent with those obtained using our previous method based upon Dirichlet/Neumann polynomials. Taking the results from the polynomial expansion given in Appendix C, substituting $t = (x_4/y_0)e^{-\frac{1}{2}x_4^2}$ and $y = \omega y_0$, retaining only terms of $O(y_0^2)$ or less, one finds agreement with the results listed in Appendix D after these have been re-expressed as a series in x_4 . This has been checked explicitly both for the background and the perturbations.

Just as in the case of the background, the small- y_0 expansion breaks down for times close to $x_4 = 1$ when the y_0^2 corrections to the perturbations become larger than the corresponding zeroth order terms. Again, we will simply analytically continue the solution in x_4 and ω around this point. In support of this, the induced metric on the positive-tension brane is, to zeroth order in y_0 , completely regular across $x_4 = 1$, even including the perturbations as can be seen from (58) and (59).

As in the case of the background, any imaginary pieces acquired from analytically continuing logarithmic terms are all suppressed by order y_0^2 . Thus they may only enter the Einstein-brane equations (when these are expanded to order y_0^2) in a linear fashion, and hence the real and imaginary parts of the metric constitute independent solutions. We can therefore simply drop the imaginary parts, or equivalently replace the $\ln(1 - x_4)$ and $\ln(1 - \omega x_4)$ terms with $\ln|1 - x_4|$ and $\ln|1 - \omega x_4|$ respectively. We have checked explicitly that this still satisfies the Einstein-brane equations and boundary conditions.

VI. COMPARISON WITH THE FOUR-DIMENSIONAL EFFECTIVE THEORY

We have now arrived at a vantage point from which we may scrutinize the predictions of the four-dimensional effective theory in light of our expansion of the bulk geometry about the scaling solution. We will find that the four-dimensional effective theory is in exact agreement with the scaling solution. Beyond this, the y_0^2 corrections lead to effects that cannot be described within a four-dimensional effective framework. Nonetheless, the higher-order corrections are automatically small at very early and very late times, restoring the accuracy of the four-dimensional effective theory in these limits.

In the near-static limit, the mapping from four to five dimensions may be calculated from the moduli space approach [2, 34, 35]: putting the four-dimensional effective theory metric $g_{\mu\nu}^4$ into Einstein frame, the mapping reads

$$g_{\mu\nu}^+ = \cosh^2(\phi/\sqrt{6})g_{\mu\nu}^4 \quad g_{\mu\nu}^- = \sinh^2(\phi/\sqrt{6})g_{\mu\nu}^4, \quad (65)$$

where $g_{\mu\nu}^+$ and $g_{\mu\nu}^-$ are the metrics on the positive- and negative-tension branes respectively, and ϕ is the radion. Two of us have shown elsewhere that on symmetry grounds this is the unique local mapping involving no derivatives [36], and that to leading order the action for $g_{\mu\nu}^4$ and ϕ is that for Einstein gravity with a minimally coupled scalar field.

Solving the four-dimensional effective theory is trivial: the background is conformally flat, $g_{\mu\nu}^4 = b_4^2(t_4)\eta_{\mu\nu}$, and the Einstein-scalar equations yield the following solution, unique up to a sign choice for ϕ_0 , of the form

$$b_4^2 = \bar{C}_4 t_4, \quad e^{\sqrt{\frac{2}{3}}\phi_0} = \bar{A}_4 t_4, \quad (66)$$

with ϕ_0 the background scalar field, and \bar{A}_4 and \bar{C}_4 arbitrary constants. (Throughout this paper we adopt units where $8\pi G_4 = 1$).

According to the map (65), the brane scale factors are then predicted to be

$$b_{\pm} = \frac{1}{2} b_4 e^{-\frac{\phi_0}{\sqrt{6}}} \left(1 \pm e^{\sqrt{\frac{2}{3}}\phi_0} \right) = 1 \pm \bar{A}_4 t_4, \quad (67)$$

where we have chosen $\bar{C}_4 = 4\bar{A}_4$, so that the brane scale factors are unity at the brane collision. As emphasized in [29], the result (67) is actually exact for the induced brane metrics, when t_4 is identified with the conformal time on the branes. From this correspondence, one can read off the five-dimensional meaning of the parameter \bar{A}_4 : it equals $L^{-1} \tanh y_0$ (our definition of y_0 differs from that of [29] by a factor of 2).

With regard to the perturbations, in longitudinal gauge (see *e.g.* [37, 38]) the perturbed line element of the four-dimensional effective theory reads

$$ds_4^2 = b_4^2(t_4) \left[-(1 + 2\Phi_4) dt_4^2 + (1 - 2\Phi_4) d\vec{x}^2 \right], \quad (68)$$

and the general solution to the perturbation equations at small k [29, 39] is

$$\Phi_4 = \frac{1}{t_4} \left(\tilde{A}_0 J_1(kt_4) + \tilde{B}_0 Y_1(kt_4) \right), \quad (69)$$

$$\frac{\delta\phi}{\sqrt{6}} = \frac{2}{3} k \left(\tilde{A}_0 J_0(kt_4) + \tilde{B}_0 Y_0(kt_4) \right) - \frac{1}{t_4} \left(\tilde{A}_0 J_1(kt_4) + \tilde{B}_0 Y_1(kt_4) \right), \quad (70)$$

with \tilde{A}_0 and \tilde{B}_0 being the amplitudes of the two linearly independent perturbation modes.

A. Background

In the case of the background, we require only the result that the scale factors on the positive- and negative-tension branes are given by

$$b_{\pm} = 1 \pm \bar{A}_4 t_4, \quad (71)$$

where the constant $\bar{A}_4 = L^{-1} \tanh y_0$ and t_4 denotes conformal time in the four-dimensional effective theory. (Note this solution has been normalized so as to set the brane scale factors at the collision to unity). Consequently, the four-dimensional effective theory restricts $b_+ + b_- = 2$. In comparison, our results from the expansion about the scaling solution (50) give

$$b_+ + b_- = 2 + \frac{2 x_4^4 (x_4^2 - 3) y_0^2}{3 (1 - x_4^2)^3} + O(y_0^4). \quad (72)$$

Thus the four-dimensional effective theory captures the behavior of the full theory only in the limit in which the y_0^2 corrections are small, *i.e.*, when the scaling solution is an accurate

description of the higher-dimensional dynamics. At small times such that $x_4 \ll 1$, the y_0^2 corrections will additionally be suppressed by $O(x_4^2)$, and so the effective theory becomes increasingly accurate in the Kaluza-Klein limit near to the collision. Close to $x_4 = 1$, the small- y_0 expansion fails hence our results for the bulk geometry is no longer reliable. For times $x_4 > 1$, the negative-tension brane no longer exists and the above expression is not defined.

We can also ask what the physical counterpart of t_4 , conformal time in the four-dimensional effective theory, is: from (50), we find

$$t_4 = \frac{b_+ - b_-}{2\bar{A}_4} = \frac{x_4}{y_0} - \frac{y_0}{30(1-x_4^2)^3} \left(x_4^3(5 - 14x_4^2 + 5x_4^4) - 5x_4(-1+x_4^2)^2 \ln(1-x_4^2) \right) + O(y_0^3). \quad (73)$$

In comparison, the physical conformal times on the positive- and negative-tension branes, defined via $b dt_{\pm} = n dt = (n/y_0)(1-x_4^2) e^{-x_4^2/2} dx_4$, are, to $O(y_0^3)$,

$$t_+ = \frac{x_4}{y_0} + \frac{y_0}{30(1-x_4^2)^3} \left(10 - 30x_4^2 - x_4^3(5 - 14x_4^2 + 5x_4^4) + 5x_4(1-x_4^2)^2 \ln(1-x_4^2) \right) \quad (74)$$

$$t_- = \frac{x_4}{y_0} - \frac{y_0}{30(1-x_4^2)^3} \left(10 - 30x_4^2 + x_4^3(5 - 14x_4^2 + 5x_4^5) - 5x_4(1-x_4^2)^2 \ln(1-x_4^2) \right), \quad (75)$$

where we have used (49) and (50).

Remarkably, to lowest order in y_0 , the two brane conformal times are in agreement not only with each other, but also with the four-dimensional effective theory conformal time. Hence, in the limit in which y_0^2 corrections are negligible, there exists a universal four-dimensional time. In this limit, $t_4 = x_4/y_0$ and the brane scale factors are simply given by $b_{\pm} = 1 \pm \bar{A}_4 t_4 = 1 \pm x_4$. The four-dimensional effective scale factor, b_4 , is given by

$$(b_4)^2 = b_+^2 - b_-^2 = 4\bar{A}_4 t_4 = 4x_4^2. \quad (76)$$

In order to describe the full five-dimensional geometry, one must specify the distance between the branes d as well as the metrics induced upon them. The distance between the branes is of particular interest in the cyclic scenario, where an inter-brane force depending on the inter-brane distance d is postulated. In the lowest approximation, where the branes are static, the four-dimensional effective theory predicts that

$$d = L \ln \coth \left(\frac{|\phi|}{\sqrt{6}} \right) = L \ln \left(\frac{b_+}{b_-} \right) = L \ln \left(\frac{1 + \bar{A}_4 t_4}{1 - \bar{A}_4 t_4} \right). \quad (77)$$

Substituting our scaling solution and evaluating to leading order in y_0 , we find

$$d = L \ln \left(\frac{1+x_4}{1-x_4} \right) + O(y_0^2). \quad (78)$$

(Again, this quantity is ill-defined for $x_4 > 1$).

In the full five-dimensional setup, a number of different measures of the inter-brane distance are conceivable, and the inter-brane force could depend upon each of these, according to the precise higher-dimensional physics. One option would be to take the metric distance along the extra dimension

$$d_m = L \int_{-y_0}^{y_0} \sqrt{g_{yy}} dy = L \int_{-y_0}^{y_0} n t dy = L \int_{-1}^1 n x_4 e^{-\frac{1}{2}x_4^2} d\omega. \quad (79)$$

Using (49), we obtain

$$d_m = L \int_{-1}^1 \frac{x_4}{1-\omega x_4} d\omega + O(y_0^2) = L \ln \left(\frac{1+x_4}{1-x_4} \right) + O(y_0^2), \quad (80)$$

in agreement with (78).

An alternative measure of the inter-brane distance is provided by considering affinely parameterized spacelike geodesics running from one brane to the other at constant Birkhoff-frame time and noncompact coordinates x^i . The background interbrane distance is just the affine parameter distance along the geodesic, and the fluctuation in distance is obtained by integrating the metric fluctuations along the geodesic, as discussed in Appendix E. One finds that, to leading order in y_0 only, the geodesic trajectories lie purely in the y -direction. Hence the affine distance d_a is trivially equal to the metric distance d_m at leading order, since

$$d_a = L \int \sqrt{g_{ab} \dot{x}^a \dot{x}^b} d\lambda = L \int n t \dot{y} d\lambda = d_m, \quad (81)$$

where the dots denote differentiation with respect to the affine parameter λ . Both measures of the inter-brane distance therefore coincide and are moreover in agreement with the four-dimensional effective theory prediction, but only at leading order in y_0 .

B. Perturbations

Since the four-dimensional Newtonian potential Φ_4 represents the *anticonformal* part of the perturbed four-dimensional effective metric (see (68)), it is unaffected by the conformal factors in (65) relating the four-dimensional effective metric to the induced brane metrics.

Hence we can directly compare the anticonformal part of the perturbations of the induced metric on the branes, as calculated in five dimensions, with $2\Phi_4$ in the four-dimensional effective theory. The induced metric on the branes is given by

$$ds^2 = b^2 \left(-(1 + 2\Phi_L) dt_{\pm}^2 + (1 - 2\Psi_L) d\vec{x}^2 \right) \quad (82)$$

$$= b^2 (1 + \Phi_L - \Psi_L) \left(-(1 + \Phi_L + \Psi_L) dt_{\pm}^2 + (1 - (\Psi_L + \Phi_L)) d\vec{x}^2 \right), \quad (83)$$

where the background brane conformal time, t_{\pm} , is related to the bulk time via $b dt_{\pm} = n dt$. The anticonformal part of the metric perturbation is thus simply $\Phi_L + \Psi_L$. It is this quantity, evaluated on the branes to leading order in y_0 , that we expect to correspond to $2\Phi_4$ in the four-dimensional effective theory.

Using our results (51) and (55) from expanding about the scaling solution, we have to $O(y_0^2)$,

$$\frac{1}{2}(\Phi_L + \Psi_L)_+ = \frac{1}{2}(\Phi_L + \Psi_L)_- = \phi_{40}(x_4) = \frac{1}{x_4} \left(A_0 J_1(\tilde{k}x_4) + B_0 Y_1(\tilde{k}x_4) \right), \quad (84)$$

with A_0 and B_0 as given in (61). On the other hand, the Newtonian potential of the four-dimensional effective theory is given by (69). Since t_4 , the conformal time in the four-dimensional effective theory, is related to the physical dimensionless brane conformal time x_4 by $t_4 = x_4/y_0$ (to lowest order in y_0), and moreover $\tilde{k} = k/y_0$, we have $\tilde{k}x_4 = kt_4$. Hence the four-dimensional effective theory prediction for the Newtonian potential is in exact agreement with the scaling solution holding at leading order in y_0 , upon identifying \tilde{A}_0 with A_0/y_0 and \tilde{B}_0 with B_0/y_0 . The behavior of the Newtonian potential is illustrated in Figure 8.

Turning our attention now to the radion perturbation, $\delta\phi$, we know from our earlier considerations that this quantity is related to the perturbation δd in the inter-brane separation. Specifically, from varying (77), we find

$$\delta d = 2L \operatorname{cosech} \left(\sqrt{\frac{2}{3}} \phi \right) \frac{\delta\phi}{\sqrt{6}}. \quad (85)$$

Inserting the four-dimensional effective theory predictions for ϕ and $\delta\phi$, we obtain

$$\frac{\delta d}{L} = \left(\frac{4\bar{A}_4 t_4}{(\bar{A}_4 t_4)^2 - 1} \right) \left(\frac{2}{3} k \left(\tilde{A}_0 J_0(kt_4) + \tilde{B}_0 Y_0(kt_4) \right) - \frac{1}{t_4} \left(\tilde{A}_0 J_1(kt_4) + \tilde{B}_0 Y_1(kt_4) \right) \right), \quad (86)$$

where to lowest order $\bar{A}_4 = y_0 + O(y_0^3)$.

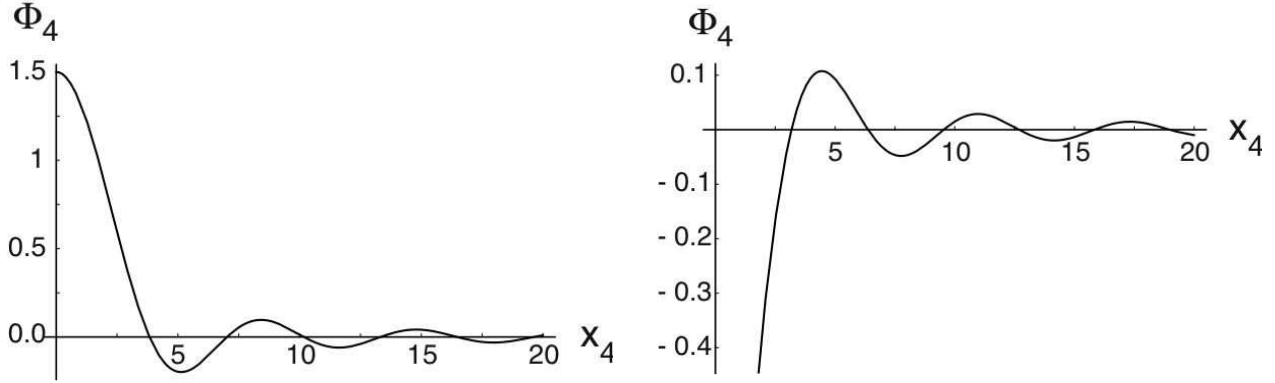


Figure 8: The four-dimensional Newtonian potential Φ_4 on the positive-tension brane, plotted to zeroth order in y_0 as a function of the time x_4 for wavelength $\tilde{k} = 1$. The plot on the left illustrates the mode with $A = 1$ and $\tilde{B} = 0$, while the plot on the right has $A = 0$ and $\tilde{B} = 1$.

In comparison, the perturbation in the metric distance between the branes is

$$\frac{\delta d_m}{L} = \int_{-y_0}^{y_0} nt \Gamma_L dy = \int_{-1}^1 \frac{nx_4 \xi_4}{b^2} e^{-\frac{1}{2}x_4^2} d\omega, \quad (87)$$

where we have used (20). Evaluating the integral using (56), to an accuracy of $O(y_0^2)$ we obtain

$$\begin{aligned} \frac{\delta d_m}{L} &= \int_{-1}^1 \frac{nx_4 \xi_{40}(x_4)}{b^2} e^{-\frac{1}{2}x_4^2} d\omega = \frac{2x_4 \xi_{40}(x_4)}{(1-x_4^2)^2} \\ &= \frac{1}{(x_4^2-1)} \left(\frac{8}{3} \tilde{k} x_4 (A_0 J_0(\tilde{k} x_4) + B_0 Y_0(\tilde{k} x_4)) - 4(A_0 J_1(\tilde{k} x_4) + B_0 Y_1(\tilde{k} x_4)) \right), \end{aligned} \quad (88)$$

which is in agreement with (86) when we set $\bar{A}_4 t_4 \sim y_0 t_4 = x_4$, along with $\tilde{A}_0 = A_0/y_0$, $\tilde{B}_0 = B_0/y_0$ and $k = \tilde{k} y_0$. The calculations in Appendix E show moreover that the perturbation in the affine distance between the branes, δd_a , is identical to the perturbation in the metric distance δd_m , to lowest order in y_0 .

The four-dimensional effective theory thus correctly predicts the Newtonian potential Φ_4 and the radion perturbation $\delta\phi$, but only in the limit in which the y_0^2 corrections are negligible and the bulk geometry is described by the scaling solution. While these corrections are automatically small at very early or very late times, at intermediate times they cannot be ignored and introduce effects that cannot be described by four-dimensional effective theory. The only five-dimensional longitudinal gauge metric perturbation we have not used in any of the above is W_L : this component is effectively invisible to the four-dimensional effective theory, since it vanishes on both branes and has no effect on the inter-brane separation.

VII. MIXING OF GROWING AND DECAYING MODES

Regardless of the rapidity of the brane collision y_0 , one expects a four-dimensional effective description to hold both near to the collision, when the brane separation is much less than an AdS length, and also when the branes are widely separated over many AdS lengths. In the former case, the warping of the bulk geometry is negligible and a Kaluza-Klein type reduction is feasible, and in the latter case, one expects to recover brane-localized gravity. At the transition between these two regions, when the brane separation is of order one AdS length, one might anticipate a breakdown of the four-dimensional effective description.

However, when the brane separation is of order a few AdS lengths, the negative-tension brane reaches the horizon of the bulk black hole and the small- y_0 expansion fails. This failure hampers any efforts to probe the breakdown of the four-dimensional effective theory at $x_4 = 1$ directly; instead, we will look for evidence of mixing between the four-dimensional perturbation modes in the transition from Kaluza-Klein to brane-localized gravity.

To see this in action we have to compare the behavior of the perturbations at very small times with that at very late times: in both of these limits a four-dimensional effective description should apply, regardless of the collision rapidity y_0 , in which the four-dimensional Newtonian potential Φ_4 satisfies

$$\Phi_4 = \frac{1}{x_4} \left(A_0 J_1(\tilde{k}x_4) + B_0 Y_1(\tilde{k}x_4) \right). \quad (89)$$

Expanding this out on long wavelengths $\tilde{k} \ll 1$, taking in addition $\tilde{k}x_4 \ll 1$, we find

$$\Phi_4 = -\frac{\tilde{B}_4^0}{x_4^2} + A_4^0 + \frac{1}{2} \tilde{B}_4^0 \tilde{k}^2 \ln \tilde{k}x_4 - \frac{1}{8} A_4^0 \tilde{k}^2 x_4^2 + O(k^4), \quad (90)$$

where the dimensionless constants A_4^0 and \tilde{B}_4^0 are given in terms of the five-dimensional perturbation amplitudes A and \tilde{B} by

$$A_4^0 = \frac{3}{2} A - \frac{9}{16} \tilde{B} - \frac{1}{8} \tilde{B} \tilde{k}^2, \quad \tilde{B}_4^0 = \frac{1}{2} \tilde{B}, \quad (91)$$

where we have used (61) and (84), recalling that $\Phi_4 = \phi_{40}$ at leading order in y_0 .

In comparison, using our results from expanding about the scaling solution, we find the

Newtonian potential on the positive-tension brane at small times $x_4 \ll 1$ is given by

$$\begin{aligned}\Phi_4 = & \left(-\frac{\tilde{B}}{2x_4^2} + \frac{3}{2}A - \frac{9}{16}\tilde{B} - \frac{1}{8}\tilde{B}\tilde{k}^2 + \frac{1}{4}\tilde{B}\tilde{k}^2 \ln \tilde{k}x_4 - \frac{3}{16}A\tilde{k}^2x_4^2 + \frac{9}{128}\tilde{B}\tilde{k}^2x_4^2 \right) \\ & + y_0^2 \left(\frac{11}{120}\tilde{B} - 3Ax_4 - \frac{47}{8}\tilde{B}x_4 - \frac{1}{2}\tilde{B}\tilde{k}^2x_4 \ln \tilde{k}x_4 + 6Ax_4^2 \right. \\ & \left. + \frac{1084}{105}\tilde{B}x_4^2 - \frac{211}{960}\tilde{B}\tilde{k}^2x_4^2 + \tilde{B}\tilde{k}^2x_4^2 \ln \tilde{k}x_4 \right) + O(x_4^3) + O(y_0^4).\end{aligned}\quad (92)$$

Examining this, we see that to zeroth order in y_0 the result is in exact agreement with (90) and (91). At y_0^2 order, however, extra terms appear that are not present in (90). Nonetheless, at sufficiently small times the effective theory is still valid as these ‘extra’ terms are subleading in x_4 : in this limit we find

$$\Phi_4 = -\frac{\tilde{B}_4^E}{x_4^2} + A_4^E + \frac{1}{2}\tilde{B}_4^E \tilde{k}^2 \ln \tilde{k}x_4 + O(x_4) + O(\tilde{k}^4) \quad (93)$$

(the superscript E indicating early times), in accordance with the four-dimensional effective theory, where

$$A_4^E = A_4^0 + \frac{11}{120}\tilde{B}y_0^2, \quad \tilde{B}_4^E = \tilde{B}_4^0. \quad (94)$$

At late times such that $x_4 \gg 1$ (but still on sufficiently long wavelengths that $\tilde{k}x_4 \ll 1$), we find on the positive-tension brane

$$\begin{aligned}\Phi_4 = & \left(-\frac{\tilde{B}}{2x_4^2} + \frac{3}{2}A - \frac{9}{16}\tilde{B} - \frac{1}{8}\tilde{B}\tilde{k}^2 + \frac{1}{4}\tilde{B}\tilde{k}^2 \ln \tilde{k}x_4 - \frac{3}{16}A\tilde{k}^2x_4^2 + \frac{9}{128}\tilde{B}\tilde{k}^2x_4^2 \right) \\ & + y_0^2 \left(-\frac{A}{3x_4^2} - \frac{\tilde{B}}{24x_4^2} - \frac{A\tilde{k}^2}{8x_4^2} + \frac{173\tilde{B}\tilde{k}^2}{960x_4^2} - \frac{\tilde{B}\tilde{k}^2 \ln \tilde{k}}{18x_4^2} - \frac{\tilde{B}\tilde{k}^2 \ln x_4}{12x_4^2} \right. \\ & \left. - \frac{3}{8}\tilde{B} + \frac{2}{9}\tilde{B}\tilde{k}^2 + \frac{1}{6}\tilde{B}\tilde{k}^2 \ln x_4 + \frac{3}{64}\tilde{B}\tilde{k}^2x_4^2 \right) + O\left(\frac{1}{x_4^3}\right) + O(y_0^4).\end{aligned}\quad (95)$$

To zeroth order in y_0 , the results again coincide with the effective theory prediction (90) and (91). However, at y_0^2 order extra terms not present in the four-dimensional effective description once more appear. In spite of this, at sufficiently late times the effective description still holds as these ‘extra’ terms are suppressed by inverse powers of x_4 relative to the leading terms, which are

$$\Phi_4 = A_4^L - \frac{\tilde{B}_4^L}{x_4^2} - \frac{1}{8}A_4^L \tilde{k}^2x_4^2 + O(\tilde{k}^2 \ln \tilde{k}x_4) \quad (96)$$

(where the superscript L indicates late times), in agreement with the four-dimensional effective theory. (Since $x_4 \gg 1$, we find $\tilde{k} \ll \tilde{k}x_4 \ll 1$, and we have chosen to retain terms of $O(\tilde{k}^2 x_4^2)$ but to drop terms of $O(\tilde{k}^2)$. The term of $O(x_4^{-2})$ is much larger than $O(\tilde{k}^2)$ and so is similarly retained). Fitting this to (95), we find [40]

$$A_4^L = A_4^0 - \frac{3}{8} \tilde{B} y_0^2, \quad \tilde{B}_4^L = \tilde{B}_4^0 + \left(\frac{A}{3} + \frac{\tilde{B}}{24} \right) y_0^2. \quad (97)$$

Comparing the amplitudes of the two four-dimensional modes at early times, A_4^E and \tilde{B}_4^E , with their counterparts A_4^L and \tilde{B}_4^L at late times, we see clearly that the amplitudes differ at y_0^2 order. Using (91), we find:

$$\begin{pmatrix} A_4^L \\ \tilde{B}_4^L \end{pmatrix} = \begin{pmatrix} 1 & -\frac{14}{15} y_0^2 \\ \frac{2}{9} y_0^2 & 1 + \left(\frac{1}{3} + \frac{\tilde{k}^2}{18} \right) y_0^2 \end{pmatrix} \begin{pmatrix} A_4^E \\ \tilde{B}_4^E \end{pmatrix}. \quad (98)$$

Hence the four-dimensional perturbation modes (as defined at very early or very late times) undergo mixing.

VIII. CONCLUSION

In this paper we have developed a set of powerful analytical methods which, we believe, render braneworld cosmological perturbation theory solvable.

Considering the simplest possible cosmological scenario, consisting of slowly-moving, flat, empty branes emerging from a collision, we have found a striking example of how the four-dimensional effective theory breaks down at first nontrivial order in the brane speed. As the branes separate, a qualitative change in the nature of the low energy modes occurs; from being nearly uniform across the extra dimension when the brane separation is small, to being exponentially localized on the positive-tension brane when the branes are widely separated. If the branes separate at finite speed, the localization process fails to keep up with the brane separation and the low energy modes do not evolve adiabatically. Instead, a given Kaluza-Klein zero mode at early times will generically evolve into a mixture of both brane-localized zero modes and excited modes in the late-time theory. From the perspective of the four-dimensional theory, this is manifested in the mixing of the four-dimensional effective perturbation modes between early and late times, as we have calculated explicitly. Such a mixing would be impossible were a local four-dimensional effective theory to remain

valid throughout cosmic history: mode-mixing is literally a signature of higher-dimensional physics, writ large across the sky.

As we show in a companion paper [21], this breakdown in the four-dimensional effective description has further ramifications for cosmology. A key quantity of interest is the comoving curvature perturbation ζ on the positive-tension brane, which is both gauge-invariant and, in the absence of additional bulk stresses, conserved on long wavelengths. We show that, at first nontrivial order in the brane speed, ζ differs from its four-dimensional effective theory analogue, ζ_4 . Hence, while the five-dimensional ζ is exactly conserved on long wavelengths in the absence of bulk stresses, the four-dimensional effective theory ζ_4 is not precisely conserved, contrary to the predictions of the four-dimensional effective theory. This has important implications for the propagation of perturbations before and after the bounce in cosmologies undergoing a big crunch/big bang transition, such as the ekpyrotic and cyclic models.

The methods developed in this paper should moreover readily extend to other braneworld models; for example those containing matter on the branes, and to models deriving from heterotic M theory which are better motivated from a fundamental perspective [26]. A further application would be to probe the dynamical evolution of braneworld black holes [41] and black strings [42] in an expanding cosmological background.

In conclusion, the strength of the expansion about the scaling solution developed in this paper lies in its ability to interpolate between very early and very late time behaviors, spanning the gap in which the effective theory fails. Not only can we solve for the full five-dimensional background and perturbations of a colliding braneworld, but our solution takes us beyond the four-dimensional effective theory and into the domain of intrinsically higher-dimensional physics.

Acknowledgments: We thank many colleagues for discussions and useful comments, especially C. de Rham, G. Gibbons, J.-L. Lehners, G. Niz, A. Tolley, S. Webster and T. Wiseman. PLM thanks PPARC and St. John's College, Cambridge, for support; NT thanks PPARC and the Darley Fellowship at Downing College, Cambridge. This work was also supported in part by US Department of Energy grant DE-FG02-91ER40671 (PJS).

Appendix A: FIVE-DIMENSIONAL LONGITUDINAL GAUGE

1. Gauge invariant variables

Starting with the background metric in the form (1), the most general scalar metric perturbation can be written as [28]

$$\begin{aligned} ds^2 = & n^2 \left(-(1 + 2\Phi) dt^2 - 2W dt dy + t^2(1 - 2\Gamma) dy^2 \right) - 2\nabla_i \alpha dx^i dt + 2t^2 \nabla_i \beta dy dx^i \\ & + b^2 ((1 - 2\Psi) \delta_{ij} - 2\nabla_i \nabla_j \chi) dx^i dx^j. \end{aligned} \quad (\text{A1})$$

Under a gauge transformation $x^A \rightarrow x^A + \xi^A$, these variables transform as

$$\begin{aligned} \Phi &\rightarrow \Phi - \dot{\xi}^t - \xi^t \frac{\dot{n}}{n} - \xi^y \frac{n'}{n}, \\ \Gamma &\rightarrow \Gamma + \xi'^y + \frac{1}{t} \xi^t + \xi^t \frac{\dot{n}}{n} + \xi^y \frac{n'}{n}, \\ W &\rightarrow W - \xi'^t + t^2 \dot{\xi}^y, \\ \alpha &\rightarrow \alpha - \xi^t + \frac{b^2}{n^2} \dot{\xi}^s, \\ \beta &\rightarrow \beta - \xi^y - \frac{b^2}{n^2 t^2} \xi'^s, \\ \Psi &\rightarrow \Psi + \xi^t \frac{\dot{b}}{b} + \xi^y \frac{b'}{b}, \\ \chi &\rightarrow \chi + \xi^s, \end{aligned} \quad (\text{A2})$$

where dots and primes indicate differentiation with respect to t and y respectively. Since a five-vector ξ^A has three scalar degrees of freedom ξ^t , ξ^y and $\xi^i = \nabla_i \xi^s$, only four of the seven functions $(\Phi, \Gamma, W, \alpha, \beta, \Psi, \chi)$ are physical. We can therefore construct four gauge-invariant variables, which are

$$\begin{aligned} \Phi_{\text{inv}} &= \Phi - \tilde{\alpha} - \tilde{\alpha} \frac{\dot{n}}{n} - \tilde{\beta} \frac{n'}{n}, \\ \Gamma_{\text{inv}} &= \Gamma + \tilde{\beta}' + \frac{1}{t} \tilde{\alpha} + \tilde{\alpha} \frac{\dot{n}}{n} + \tilde{\beta} \frac{n'}{n}, \\ W_{\text{inv}} &= W - \tilde{\alpha}' + t^2 \dot{\tilde{\beta}}, \\ \Psi_{\text{inv}} &= \Psi + \frac{\dot{b}}{b} \tilde{\alpha} + \frac{b'}{b} \tilde{\beta}, \end{aligned} \quad (\text{A3})$$

where $\tilde{\alpha} = \alpha - \frac{b^2}{n^2} \dot{\chi}$ and $\tilde{\beta} = \beta + \frac{b^2}{n^2 t^2} \chi'$.

In analogy with the four-dimensional case, we then define five-dimensional longitudinal

gauge by $\chi = \alpha = \beta = 0$, giving

$$\begin{aligned}\Phi_{\text{inv}} &= \Phi_L, \\ \Gamma_{\text{inv}} &= \Gamma_L, \\ W_{\text{inv}} &= W_L, \\ \Psi_{\text{inv}} &= \Psi_L,\end{aligned}\tag{A4}$$

i.e. the gauge-invariant variables are equal to the values of the metric perturbations in longitudinal gauge. This gauge is spatially isotropic in the x^i coordinates, although in general there will be a non-zero t - y component of the metric.

2. Position of branes

In general, the locations of the branes will be different for different choices of gauge. In the case where the brane matter has no anisotropic stresses this is easy to establish. Working out the Israel matching conditions, we find that β on the branes is related to the anisotropic part of the brane's stress-energy. If we consider only perfect fluids, for which the shear vanishes, then the Israel matching conditions give $\beta(y = \pm y_0) = 0$.

From the gauge transformations above, we can transform into the gauge $\alpha = \chi = 0$ using only a ξ^s and a ξ^t transformation. We may then pass to longitudinal gauge ($\alpha = \beta = \chi = 0$) with the transformation $\xi^y = \tilde{\beta}$ alone. Since β (and hence $\tilde{\beta}$) vanishes on the branes, ξ^y must also vanish leaving the brane trajectories unperturbed. Hence, in longitudinal gauge the brane locations remain at their unperturbed values $y = \pm y_0$. Transforming to a completely arbitrary gauge, we see that in general the brane locations are given by

$$y = \pm y_0 - \tilde{\beta}.\tag{A5}$$

Appendix B: POLYNOMIAL EXPANSION: BACKGROUND

Using the expansion in Dirichlet/Neumann polynomials presented in Section IV to solve for the background geometry, we find

$$\begin{aligned} N_0 &= \frac{1}{t} - \frac{1}{2} t y_0^2 + \frac{1}{24} t (8 - 9 t^2) y_0^4 - \frac{1}{720} t (136 + 900 t^2 + 375 t^4) y_0^6 \\ &\quad + \frac{1}{40320} t (3968 + 354816 t^2 - 348544 t^4 - 36015 t^6) y_0^8 + O(y_0^{10}) \end{aligned} \quad (B1)$$

$$\begin{aligned} N_3 &= -\frac{1}{6} + \left(\frac{5}{72} - 2 t^2 \right) y_0^2 - \frac{1}{2160} (61 - 20880 t^2 + 19440 t^4) y_0^4 \\ &\quad + \left(\frac{277}{24192} - \frac{743 t^2}{20} + \frac{677 t^4}{6} - \frac{101 t^6}{3} \right) y_0^6 + O(y_0^8) \end{aligned} \quad (B2)$$

$$N_4 = \frac{3 t^3 y_0^2}{2} + \frac{t^3 (-28 + 33 t^2) y_0^4}{4} + \frac{t^3 (1984 - 6776 t^2 + 2715 t^4) y_0^6}{80} + O(y_0^8) \quad (B3)$$

$$\begin{aligned} N_5 &= -\frac{1}{120} - \frac{(-7 + 1800 t^2 + 540 t^4) y_0^2}{1800} \\ &\quad - \frac{(323 - 990528 t^2 + 2207520 t^4 + 362880 t^6) y_0^4}{201600} + O(y_0^6) \end{aligned} \quad (B4)$$

$$N_6 = t^3 y_0^2 + \frac{1}{30} t^3 (-142 + 371 t^2) y_0^4 + O(y_0^6) \quad (B5)$$

$$N_7 = -\frac{1}{5040} - \frac{(-9 + 20384 t^2 + 23520 t^4) y_0^2}{94080} + O(y_0^4) \quad (B6)$$

$$N_8 = \frac{3 t^3 y_0^2}{10} + O(y_0^4) \quad (B7)$$

$$N_9 = \frac{1}{362880} + O(y_0^2) \quad (B8)$$

$$N_{10} = O(y_0^2) \quad (B9)$$

and

$$\begin{aligned} q_0 &= 1 - \frac{3 t^2 y_0^2}{2} + \left(t^2 - \frac{7 t^4}{8} \right) y_0^4 + \left(\frac{-17 t^2}{30} + \frac{17 t^4}{12} - \frac{55 t^6}{48} \right) y_0^6 \\ &\quad + \left(\frac{31 t^2}{105} - \frac{9 t^4}{5} + \frac{233 t^6}{90} - \frac{245 t^8}{128} \right) y_0^8 + O(y_0^{10}) \end{aligned} \quad (B10)$$

$$q_3 = -2 t^3 y_0^2 + \left(\frac{29 t^3}{3} - 8 t^5 \right) y_0^4 + \left(-\frac{743 t^3}{20} + \frac{322 t^5}{3} - 27 t^7 \right) y_0^6 + O(y_0^8) \quad (B11)$$

$$q_4 = \frac{t^4 y_0^2}{2} + \left(\frac{-5 t^4}{3} + \frac{9 t^6}{4} \right) y_0^4 + O(y_0^6) \quad (B12)$$

$$q_5 = -t^3 y_0^2 + \left(\frac{737 t^3}{150} - \frac{58 t^5}{5} \right) y_0^4 + O(y_0^6) \quad (B13)$$

$$q_6 = \frac{t^4 y_0^2}{3} + O(y_0^4) \quad (B14)$$

$$q_7 = \frac{-13 t^3 y_0^2}{60} + O(y_0^4) \quad (B15)$$

$$q_8 = O(y_0^2) \quad (B16)$$

$$q_9 = O(y_0^2), \quad (B17)$$

where we have set $L = 1$ for clarity. (To restore L simply replace $t \rightarrow t/L$). The solution has been checked to satisfy all the remaining Einstein equations explicitly.

Appendix C: POLYNOMIAL EXPANSION: PERTURBATIONS

1. All wavelengths

Throughout this Appendix, we shall set the AdS radius L to unity. It is then simple to restore L by dimensions where needed, *i.e.* by setting $t \rightarrow t/L$ and $k \rightarrow kL$. Note that the coordinate y is dimensionless.

Using the Dirichlet/Neumann polynomial expansion to solve for the perturbations, the solution may be expressed in terms of the original longitudinal gauge variables as

$$\Phi_L = \mathcal{P}_\Phi^{(0)}(y, t) F^{(0)}(t) + \mathcal{P}_\Phi^{(1)}(y, t) F^{(1)}(t) \quad (C1)$$

where

$$F^{(n)}(t) = \bar{A} J_n(kt) + \bar{B} Y_n(kt) \quad (C2)$$

for $n = 0, 1$ and $\gamma = 0.577 \dots$ is the Euler-Mascheroni constant. The constants \bar{A} and \bar{B} are arbitrary functions of k . In order to be consistent with the series expansion in t presented in Section III, we must set

$$\bar{A} = 12 A + 2 B k^2 (\ln 2 - \gamma) - \frac{9 B y_0^2}{2} + \frac{233 B y_0^4}{45} + O(y_0^6) \quad (C3)$$

$$\bar{B} = B k^2 \pi + O(y_0^6). \quad (C4)$$

The polynomials $\mathcal{P}_\Phi^{(n)}$ are then given (for all k and t) by

$$\begin{aligned}
\mathcal{P}_\Phi^{(0)}(t, y) = & -\frac{1}{6} + \frac{t y}{3} + \frac{t^2 (-2 y^2 + y_0^2)}{12} + \frac{t y (11 y^2 + 3 (-11 + 3 t^2) y_0^2)}{36} + \\
& \frac{t^2 (-525 y^4 + 90 (19 - 5 t^2) y^2 y_0^2 + (511 - 180 t^2 + 45 k^2 t^4) y_0^4)}{2160} - \\
& \frac{t y}{2160} \left(3 (-92 + (9 + 4 k^2) t^2) y^4 + 30 (92 - (219 + 4 k^2) t^2 + k^2 t^4) y^2 y_0^2 + \right. \\
& \left. (-6900 + (20087 + 300 k^2) t^2 - 90 (13 + k^2) t^4 + 90 k^2 t^6) y_0^4 \right) + O(y_0^6), \\
\end{aligned} \tag{C5}$$

$$\begin{aligned}
\mathcal{P}_\Phi^{(1)}(t, y) = & \frac{1}{k t} \left[\frac{1}{2} - \frac{t y}{2} + \frac{t^2 (3 y^2 + (-3 + k^2 t^2) y_0^2)}{12} - \right. \\
& \frac{t y ((3 + k^2 t^2) y^2 + 3 (-3 + (3 - k^2) t^2 + 2 k^2 t^4) y_0^2)}{36} + \\
& \frac{t^2}{2160} \left(75 (6 + k^2 t^2) y^4 + 90 (-12 + 3 (2 - k^2) t^2 + 2 k^2 t^4) y^2 y_0^2 + \right. \\
& \left. (718 + k^2 t^2 (-101 + 225 t^2)) y_0^4 \right) - \\
& \frac{t y}{2160} \left(3 (3 + 2 (-9 + 31 k^2) t^2 + 2 k^2 t^4) y^4 + \right. \\
& 30 (-3 + (219 - 62 k^2) t^2 + 16 k^2 t^4) y^2 y_0^2 + \\
& \left. \left. (225 + (-20104 + 4650 k^2) t^2 + (1215 - 1822 k^2) t^4 + 765 k^2 t^6) y_0^4 \right) \right] \\
& + O(y_0^6). \\
\end{aligned} \tag{C6}$$

Since the $F^{(n)}$ are of zeroth order in y_0 , the solution for Φ_L to a given order less than $O(y_0^6)$ is found simply by truncating the polynomials above. (Should they be needed, results up to $O(y_0^{14})$ can in addition be found at [27]).

In a similar fashion we may express the solution for Ψ_L as

$$\Psi_L = \mathcal{P}_\Psi^{(0)}(y, t) F^{(0)}(t) + \mathcal{P}_\Psi^{(1)}(y, t) F^{(1)}(t), \tag{C7}$$

where $F^{(n)}$ is defined as above and

$$\begin{aligned} \mathcal{P}_{\Psi}^{(0)}(t, y) = & \frac{1}{6} - \frac{t y}{3} + \frac{t^2 (y^2 + y_0^2)}{6} + \frac{t y (-2 y^2 + 3 (2 - 3 t^2) y_0^2)}{36} + \\ & \frac{t^2 (120 y^4 + 450 (-2 + t^2) y^2 y_0^2 + (644 + 450 t^2 - 45 k^2 t^4) y_0^4)}{2160} + \\ & \frac{t y}{2160} \left(3 (-2 + (9 + 4 k^2) t^2) y^4 + 30 (2 + 4 (9 - k^2) t^2 + k^2 t^4) y^2 y_0^2 + \right. \\ & \left. (-150 + (-2863 + 300 k^2) t^2 - 90 (13 + k^2) t^4 + 90 k^2 t^6) y_0^4 \right) + O(y_0^6), \end{aligned} \quad (C8)$$

$$\begin{aligned} \mathcal{P}_{\Psi}^{(1)}(t, y) = & \frac{1}{k t} \left[\frac{t y}{2} - \frac{t^2 (3 y^2 + (3 + k^2 t^2) y_0^2)}{12} + \right. \\ & \frac{t y ((3 + k^2 t^2) y^2 + 3 (-3 + (3 - k^2) t^2 + 2 k^2 t^4) y_0^2)}{36} - \\ & \frac{t^2}{2160} \left(15 (12 + 5 k^2 t^2) y^4 + 90 (-6 - 3 (-2 + k^2) t^2 + 2 k^2 t^4) y^2 y_0^2 + \right. \\ & \left. (-752 + (540 - 101 k^2) t^2 + 360 k^2 t^4) y_0^4 \right) + \\ & \frac{t y}{2160} \left((9 + 6 (-9 + k^2) t^2 + 6 k^2 t^4) y^4 + \right. \\ & 30 (-3 - (33 + 2 k^2) t^2 + 7 k^2 t^4) y^2 y_0^2 + \\ & \left. (225 + 2 (1288 + 75 k^2) t^2 + (1215 - 1012 k^2) t^4 + 765 k^2 t^6) y_0^4 \right) \\ & + O(y_0^6). \end{aligned} \quad (C9)$$

Finally, writing

$$W_L = \mathcal{P}_W^{(0)}(y, t) F^{(0)}(t) + \mathcal{P}_W^{(1)}(y, t) F^{(1)}(t), \quad (C10)$$

we find

$$\begin{aligned} \mathcal{P}_W^{(0)}(t, y) = & -\frac{1}{60} t^2 (y^2 - y_0^2) \left(-30 + 30 t y - 25 (y^2 + (-5 + 3 t^2) y_0^2) + \right. \\ & \left. t y (21 y^2 + (-149 + 75 t^2) y_0^2) \right) + O(y_0^6), \end{aligned} \quad (C11)$$

$$\begin{aligned} \mathcal{P}_W^{(1)}(t, y) = & -\frac{1}{60 k} t^2 (y^2 - y_0^2) \left(30 y - 5 k^2 t (2 y^2 + (-10 + 3 t^2) y_0^2) + \right. \\ & \left. y ((12 + 11 k^2 t^2) y^2 + (-38 + (60 - 69 k^2) t^2 + 15 k^2 t^4) y_0^2) \right) + O(y_0^6). \end{aligned} \quad (C12)$$

2. Long wavelengths

On long wavelengths, $F^{(n)}$ reduces to

$$F^{(0)}(t) = 12A - \frac{9B y_0^2}{2} + \frac{233B y_0^4}{45} + O(k^2) + O(y_0^6), \quad (\text{C13})$$

$$F^{(1)}(t) = \left(6At - \left(\frac{2}{t} + \frac{9t y_0^2}{4} - \frac{233t y_0^4}{90} \right) B \right) k + O(k^2) + O(y_0^6). \quad (\text{C14})$$

For convenience, we provide here a separate listing of the metric perturbations truncated at $O(k^2)$:

$$\begin{aligned} \Phi_L = & \left(A - \frac{B}{t^2} \right) + \left(\frac{By}{t} + At y \right) + \frac{1}{8} \left(B(y_0^2 - 4y^2) - 4At^2(y_0^2 + y^2) \right) \\ & + \frac{y}{24t} \left(B(3y_0^2(-4 + t^2) + 4y^2) + 4At^2(3y_0^2(-19 + 3t^2) + 19y^2) \right) \\ & + \left(\frac{1}{6}At^2(y_0^4(29 - 6t^2) + 3y_0^2(13 - 2t^2)y^2 - 10y^4) \right. \\ & \left. - \frac{1}{240}(B(y_0^4(56 - 45t^2) + 15y_0^2(-16 + 5t^2)y^2 + 100y^4)) \right) \\ & + \frac{y}{240t} \left(2At^2(5y_0^4(905 - 1338t^2 + 75t^4) + 10y_0^2(-181 + 219t^2)y^2 + 181y^4) \right. \\ & \left. + B(y_0^4(50 - 3509t^2 + 135t^4) + 5y_0^2(-4 + 235t^2)y^2 + (2 - 12t^2)y^4) \right) \\ & + O(y_0^6), \end{aligned} \quad (\text{C15})$$

$$\begin{aligned} \Psi_L = & 2A - \frac{y}{t}(B + At^2) + \frac{1}{4} \left(2At^2(y_0^2 + y^2) + B(-y_0^2 + 2y^2) \right) \\ & - \frac{y}{24t} \left(4At^2(3y_0^2(-1 + 3t^2) + y^2) + B(3y_0^2(-4 + t^2) + 4y^2) \right) \\ & + \frac{1}{48} \left(8At^2(2y_0^4(17 + 3t^2) + 3y_0^2(-7 + 2t^2)y^2 + y^4) \right. \\ & \left. + B(y_0^4(8 + 15t^2) + 3y_0^2(-8 + 5t^2)y^2 + 8y^4) \right) \\ & - \frac{y}{240t} \left(2At^2(25y_0^4(1 + 42t^2 + 15t^4) - 10y_0^2(1 + 39t^2)y^2 + y^4) \right. \\ & \left. + B(y_0^4(50 + 721t^2 + 135t^4) - 5y_0^2(4 + 47t^2)y^2 + (2 - 12t^2)y^4) \right) \\ & + O(y_0^6), \end{aligned} \quad (\text{C16})$$

$$\begin{aligned} W_L = & 6At^2(-y_0^2 + y^2) - t(B + 3At^2)y(-y_0^2 + y^2) \\ & + \frac{1}{4}t^2(-y_0^2 + y^2)(-9By_0^2 + 20A(y_0^2(-5 + 3t^2) + y^2)) \\ & - \frac{1}{120}ty(-y_0^2 + y^2)(120At^2(y_0^2(-26 + 9t^2) + 3y^2) \\ & + B(y_0^2(-152 + 105t^2) + 48y^2)) + O(y_0^6). \end{aligned} \quad (\text{C17})$$

Terms up to $O(y_0^{14})$ are available at [27].

Appendix D: PERTURBATIONS FROM EXPANSION ABOUT THE SCALING SOLUTION

Following the method presented in Section V, the perturbations were computed to $O(y_0^4)$. On long wavelengths, the five-dimensional longitudinal gauge variables take the form

$$\Phi_L = f_0^\Phi + y_0^2(f_1^\Phi + f_2^\Phi \ln(1+x_4) + f_3^\Phi \ln(1-x_4) + f_4^\Phi \ln(1-\omega x_4)), \quad (D1)$$

$$\Psi_L = f_0^\Psi + y_0^2(f_1^\Psi + f_2^\Psi \ln(1+x_4) + f_3^\Psi \ln(1-x_4) + f_4^\Psi \ln(1-\omega x_4)), \quad (D2)$$

$$W_L = e^{-\frac{1}{2}x_4^2} (f_0^W + y_0^2(f_1^W + f_2^W \ln(1+x_4) + f_3^W \ln(1-x_4) + f_4^W \ln(1-\omega x_4))), \quad (D3)$$

where the f are rational functions of x_4 and ω . For Φ_L , we have

$$\begin{aligned} f_0^\Phi &= \frac{1}{16x_4^2(-1+x_4^2)} \left(16\tilde{B} - 16\tilde{B}\omega x_4 - 2(8A + \tilde{B} - 4\tilde{B}\omega^2)x_4^2 + 2(-8A + 3\tilde{B})\omega x_4^3 \right. \\ &\quad \left. + (8A - 3\tilde{B})(3 + \omega^2)x_4^4 \right), \end{aligned} \quad (D4)$$

$$\begin{aligned} f_1^\Phi &= \frac{1}{960x_4^4(-1+x_4^2)^5} \left(8Ax_4^5 \left(-580x_4 + 95x_4^3 - 576\omega^5x_4^4 + 281x_4^5 + 96\omega^6x_4^5 - 60x_4^7 \right. \right. \\ &\quad \left. \left. + 5\omega^4x_4(40 + 167x_4^2 - 39x_4^4) + 20\omega^3(-19 - 5x_4^2 + 48x_4^4) \right. \right. \\ &\quad \left. \left. + 10\omega^2x_4(-78 - 117x_4^2 + x_4^4 + 2x_4^6) + 4\omega(285 + 100x_4^2 - 25x_4^4 - 29x_4^6 + 5x_4^8) \right) \right. \\ &\quad \left. + \tilde{B} \left(-1920 + x_4(480\omega + 80(91 + 15\omega^2)x_4 \right. \right. \\ &\quad \left. \left. - 160\omega(5 + 4\omega^2)x_4^2 + 40(-273 - 116\omega^2 + 7\omega^4)x_4^3 - 20\omega(-649 + 127\omega^2)x_4^4 \right. \right. \\ &\quad \left. \left. + 4(1231 - 3285\omega^2 + 2060\omega^4)x_4^5 - 4\omega(2036 - 2115\omega^2 + 1152\omega^4)x_4^6 \right. \right. \\ &\quad \left. \left. + (1107 + 8102\omega^2 - 4905\omega^4 + 768\omega^6)x_4^7 + 12\omega(233 + 48\omega^2(-5 + 3\omega^2))x_4^8 \right. \right. \\ &\quad \left. \left. - (3131 + 1582\omega^2 - 585\omega^4 + 288\omega^6)x_4^9 - 772\omega x_4^{10} + 20(85 + 29\omega^2)x_4^{11} \right. \right. \\ &\quad \left. \left. + 180\omega x_4^{12} - 120(3 + \omega^2)x_4^{13}) \right) \right), \end{aligned} \quad (D5)$$

$$\begin{aligned} f_2^\Phi &= \frac{1}{48x_4^5(-1+x_4^2)^3} \left(\tilde{B} \left(48 + (36 - 48\omega)x_4 + 12(-7 - 6\omega + 2\omega^2)x_4^2 \right. \right. \\ &\quad \left. \left. + 4(-13 + 6\omega + 9\omega^2)x_4^3 + (60 + 80\omega - 12\omega^2)x_4^4 - 4(-8 - 6\omega + 9\omega^2)x_4^5 \right. \right. \\ &\quad \left. \left. - 3(8 + 7\omega + 4\omega^2)x_4^6 + (-11 + 5\omega^2)x_4^7 + 3\omega x_4^8 \right) + 8Ax_4^6(x_4 + \omega^2 x_4 \right. \\ &\quad \left. - \omega(1 + x_4^2)) \right), \end{aligned} \quad (D6)$$

$$\begin{aligned}
f_3^\Psi &= \frac{1}{48x_4^5(-1+x_4^2)^3} \left(\tilde{B} \left(-48 + 12(3+4\omega)x_4 - 12(-7+6\omega+2\omega^2)x_4^2 \right. \right. \\
&\quad + 4(-13-6\omega+9\omega^2)x_4^3 + 4(-15+20\omega+3\omega^2)x_4^4 - 4(-8+6\omega+9\omega^2)x_4^5 \\
&\quad \left. \left. + 3(8-7\omega+4\omega^2)x_4^6 + (-11+5\omega^2)x_4^7 + 3\omega x_4^8 \right) \right. \\
&\quad \left. + 8Ax_4^6(x_4 + \omega^2 x_4 - \omega(1+x_4^2)) \right), \tag{D7}
\end{aligned}$$

$$f_4^\phi = \frac{3\tilde{B}(-1+\omega x_4)^2}{2x_4^4(-1+x_4^2)^2}. \tag{D8}$$

Similarly, for Ψ_L , we find

$$\begin{aligned}
f_0^\Psi &= \frac{1}{16x_4(-1+x_4^2)} \left(16\tilde{B}\omega - 4(8A + \tilde{B}(-1+2\omega^2))x_4 + 2(8A - 3\tilde{B})\omega x_4^2 \right. \\
&\quad \left. + (-8A + 3\tilde{B})(-3 + \omega^2)x_4^3 \right), \tag{D9}
\end{aligned}$$

$$\begin{aligned}
f_1^\Psi &= \frac{1}{960x_4^3(-1+x_4^2)^5} \left(-480\tilde{B}\omega - 240\tilde{B}(-7+5\omega^2)x_4 + 160\tilde{B}\omega(5+4\omega^2)x_4^2 \right. \\
&\quad - 40\tilde{B}(143-104\omega^2+\omega^4)x_4^3 + 20\omega(\tilde{B}(197-155\omega^2) + 8A(-3+\omega^2))x_4^4 \\
&\quad + 20(-8A(34-21\omega^2+\omega^4) + \tilde{B}(98-369\omega^2+101\omega^4))x_4^5 \\
&\quad - 4\omega(200A(-14+5\omega^2) + \tilde{B}(34-975\omega^2+288\omega^4))x_4^6 + (40A(55-234\omega^2+67\omega^4) \\
&\quad + \tilde{B}(2455+838\omega^2-1005\omega^4+192\omega^6))x_4^7 - 4\omega(3\tilde{B}(53+120\omega^2-36\omega^4) \\
&\quad + 8A(155-120\omega^2+36\omega^4))x_4^8 + (\tilde{B}(-3515+1042\omega^2+225\omega^4-72\omega^6) \\
&\quad + 8A(89+170\omega^2-75\omega^4+24\omega^6))x_4^9 + 4(232A+193\tilde{B})\omega x_4^{10} - 20(8A(1+\omega^2) \\
&\quad + \tilde{B}(-91+29\omega^2))x_4^{11} - 20(8A+9\tilde{B})\omega x_4^{12} + 120\tilde{B}(-3+\omega^2)x_4^{13} \right), \tag{D10}
\end{aligned}$$

$$\begin{aligned}
f_2^\Psi &= \frac{-1}{48x_4^4(-1+x_4^2)^3} \left(8Ax_4^5(x_4 + \omega^2 x_4 - \omega(1+x_4^2)) + \tilde{B}(36+60x_4-36x_4^2-84x_4^3+ \right. \\
&\quad 24x_4^5+5x_4^6+\omega^2 x_4(24+36x_4-12x_4^2-36x_4^3-12x_4^4+5x_4^5) \\
&\quad \left. + \omega(-48-72x_4+24x_4^2+80x_4^3+24x_4^4-21x_4^5+3x_4^7)) \right), \tag{D11}
\end{aligned}$$

$$\begin{aligned}
f_3^\Psi &= \frac{1}{48x_4^4(-1+x_4^2)^3} \left(8Ax_4^5(-x_4 - \omega^2 x_4 + \omega(1+x_4^2)) + \tilde{B}(-36+60x_4+36x_4^2- \right. \\
&\quad 84x_4^3+24x_4^5-5x_4^6-\omega^2 x_4(-24+36x_4+12x_4^2-36x_4^3+12x_4^4+5x_4^5) \\
&\quad \left. + \omega(-48+72x_4+24x_4^2-80x_4^3+24x_4^4+21x_4^5-3x_4^7)) \right), \tag{D12}
\end{aligned}$$

$$f_4^\Psi = \frac{-3\tilde{B}(-1+\omega x_4)^2}{2x_4^4(-1+x_4^2)^2}. \tag{D13}$$

Finally, for W_L , we have

$$f_0^W = \frac{(-1 + \omega^2)x_4(-24Ax_4(-2 + \omega x_4) + \tilde{B}(-18x_4 + \omega(-8 + 9x_4^2)))}{8(-1 + x_4^2)^2}, \quad (\text{D14})$$

$$\begin{aligned} f_1^W = & \frac{(-1 + \omega^2)}{480x_4^2(-1 + x_4^2)^7} \left(8Ax_4^4(1500 + 84\omega^4x_4^4(-12 + x_4^2) \right. \\ & - 6\omega^2(50 + 100x_4^2 - 427x_4^4 + x_4^6) + 3\omega^3x_4(60 + 585x_4^2 - 160x_4^4 + 3x_4^6) \\ & + \omega^5(168x_4^5 - 36x_4^7) - 6x_4^2(-590 + 243x_4^2 + 201x_4^4 - 4x_4^6 + 10x_4^8) \\ & + \omega x_4(-1560 - 4935x_4^2 + 2000x_4^4 - 265x_4^6 + 92x_4^8) \\ & + \tilde{B}(1440 + x_4(-84\omega^4x_4^5(24 + 28x_4^2 + 3x_4^4) \\ & + 12\omega^5x_4^6(40 + 6x_4^2 + 9x_4^4) + 6\omega^2x_4^3(-450 + 964x_4^2 + 863x_4^4 + 3x_4^6) \\ & - 3\omega^3x_4^2(-40 - 748x_4^2 - 2333x_4^4 + 672x_4^6 + 9x_4^8) \\ & - 6x_4(2160 - 5490x_4^2 + 3770x_4^4 - 2249x_4^6 + 597x_4^8 - 588x_4^{10} + 90x_4^{12}) \\ & + \omega(-2160 + 18920x_4^2 - 53216x_4^4 + 20629x_4^6 - 11216x_4^8 + 5579x_4^{10} \\ & \left. - 2236x_4^{12} + 360x_4^{14})) \right), \quad (\text{D15}) \end{aligned}$$

$$\begin{aligned} f_2^W = & \frac{(1 - \omega)}{24(x_4 - x_4^3)^4} \left(\tilde{B}(-144 + 108(-1 + 2\omega)x_4 - 24(-5 + \omega)(3 + 2\omega)x_4^2 \right. \\ & - 36(-11 + \omega(16 + \omega))x_4^3 + 24\omega(-29 + 7\omega)x_4^4 \\ & + 36(-2 + \omega(-2 + 7\omega))x_4^5 + 3(1 + \omega)(3 + 32\omega)x_4^6 + 7\omega(1 + \omega)x_4^7 \\ & \left. + 27(1 + \omega)x_4^8 - 9\omega(1 + \omega)x_4^9) + 24A(1 + \omega)x_4^6(-1 - 3x_4^2 + \omega(x_4 + x_4^3)) \right), \quad (\text{D16}) \end{aligned}$$

$$\begin{aligned} f_3^W = & \frac{(1 + \omega)}{24x_4^4(-1 + x_4^2)^4} \left(\tilde{B}(-144 + 108(1 + 2\omega)x_4 - 24(5 + \omega)(-3 + 2\omega)x_4^2 \right. \\ & + 36(-11 + (-16 + \omega)\omega)x_4^3 + 24\omega(29 + 7\omega)x_4^4 - 36(-2 + \omega(2 + 7\omega))x_4^5 \\ & + 3(-1 + \omega)(-3 + 32\omega)x_4^6 - 7(-1 + \omega)\omega x_4^7 - 27(-1 + \omega)x_4^8 \\ & \left. + 9(-1 + \omega)\omega x_4^9) - 24A(-1 + \omega)x_4^6(-1 - 3x_4^2 + \omega(x_4 + x_4^3)) \right), \quad (\text{D17}) \end{aligned}$$

$$f_4^W = \frac{3\tilde{B}(-1 + \omega x_4)^2(4 - 10x_4^2 + \omega x_4(-1 + 7x_4^2))}{x_4^4(-1 + x_4^2)^4}. \quad (\text{D18})$$

Results including the \tilde{k}^2 corrections can be found at [27].

Appendix E: BULK GEODESICS

To calculate the affine distance between the branes along a spacelike geodesic we must solve the geodesic equations in the bulk. Let us first consider the situation in Birkhoff-frame coordinates for which the bulk metric is static and the branes are moving. The Birkhoff-frame metric takes the form [29]

$$ds^2 = dY^2 - N^2(Y) dT^2 + A^2(Y) d\vec{x}^2, \quad (E1)$$

where for Schwarzschild-AdS with a horizon at $Y = 0$,

$$A^2(Y) = \frac{\cosh(2Y/L)}{\cosh(2Y_0/L)}, \quad N^2(Y) = \frac{\cosh(2Y_0/L)}{\cosh(2Y/L)} \left(\frac{\sinh(2Y/L)}{\sinh(2Y_0/L)} \right)^2. \quad (E2)$$

At $T = 0$, the Y -coordinate of the branes is represented by the parameter Y_0 ; their subsequent trajectories $Y_{\pm}(T)$ can then be determined by integrating the Israel matching conditions, which read $\tanh(2Y_{\pm}/L) = \pm\sqrt{1 - V_{\pm}^2}$, where $V_{\pm} = (dY_{\pm}/dT)/N(Y_{\pm})$ are the proper speeds of the positive- and negative-tension branes respectively. From this, it further follows that Y_0 is related to the rapidity y_0 of the collision by $\tanh y_0 = \operatorname{sech}(2Y_0/L)$.

For the purpose of measuring the distance between the branes, a natural choice is to use spacelike geodesics that are orthogonal to the four translational Killing vectors of the static bulk, corresponding to shifts in \vec{x} and T . Taking the \vec{x} and T coordinates to be fixed along the geodesic then, we find that $Y_{,\lambda}$ is constant for an affine parameter λ along the geodesic.

To make the connection to our original brane-static coordinate system, recall that the metric function $b^2(t, y) = A^2(Y)$, and thus

$$Y_{,\lambda}^2 = \frac{(bb_{,t}t_{,\lambda} + bb_{,y}y_{,\lambda})^2}{b^4 - \theta^2} = n^2(-t_{,\lambda}^2 + t^2y_{,\lambda}^2), \quad (E3)$$

where we have introduced the constant $\theta = \tanh y_0 = V/c$. Adopting y now as the affine parameter, we have

$$0 = (b_{,t}^2 b^2 + n^2(b^4 - \theta^2))t_{,y}^2 + 2b_{,t}b_{,y}b^2t_{,y} + (b_{,y}^2 b^2 - n^2t^2(b^4 - \theta^2)), \quad (E4)$$

where t is to be regarded now as a function of y .

We can solve this equation order by order in y_0 using the series ansatz

$$t(y) = \sum_{n=0}^{\infty} c_n y^n, \quad (E5)$$

where the constants c_n are themselves series in y_0 . Using the series solution for the background geometry given in Appendix B, and imposing the boundary condition that $t(y_0) = t_0$, we obtain

$$c_0 = t_0 + \frac{t_0 y_0^2}{2} - 2 t_0^2 y_0^3 + \frac{(t_0 + 36 t_0^3) y_0^4}{24} - t_0^2 (1 + 5 t_0^2) y_0^5 + \left(\frac{t_0}{720} + \frac{17 t_0^3}{4} + 4 t_0^5 \right) y_0^6 - \frac{t_0^2 (13 + 250 t_0^2 + 795 t_0^4) y_0^7}{60} + O(y_0^8) \quad (\text{E6})$$

$$c_1 = 2 t_0^2 y_0^2 + \left(\frac{5 t_0^2}{3} + 5 t_0^4 \right) y_0^4 - 8 t_0^3 y_0^5 + \left(\frac{91 t_0^2}{180} + \frac{23 t_0^4}{6} + \frac{53 t_0^6}{4} \right) y_0^6 + O(y_0^7) \quad (\text{E7})$$

$$c_2 = -\frac{t_0}{2} - \frac{t_0 (1 + 6 t_0^2) y_0^2}{4} + t_0^2 y_0^3 - \left(\frac{t_0}{48} - 2 t_0^3 + 4 t_0^5 \right) y_0^4 + \frac{(t_0^2 + 23 t_0^4) y_0^5}{2} + O(y_0^6) \quad (\text{E8})$$

$$c_3 = -\frac{5 t_0^2 y_0^2}{3} - \frac{t_0^2 (25 + 201 t_0^2) y_0^4}{18} + O(y_0^5) \quad (\text{E9})$$

$$c_4 = \frac{5 t_0}{24} + \left(\frac{5 t_0}{48} + \frac{7 t_0^3}{4} \right) y_0^2 - \frac{5 t_0^2 y_0^3}{12} + O(y_0^4) \quad (\text{E10})$$

$$c_5 = \frac{61 t_0^2 y_0^2}{60} + O(y_0^3) \quad (\text{E11})$$

$$c_6 = -\frac{61 t_0}{720} + O(y_0^2) \quad (\text{E12})$$

$$c_7 = 0 + O(y_0). \quad (\text{E13})$$

Substituting $t_0 = x_0/y_0$ and $y = \omega y_0$ we find $x(\omega) = x_0/y_0 + O(y_0)$, *i.e.* to lowest order in y_0 , the geodesics are trajectories of constant time lying solely along the ω direction. Hence in this limit, the affine and metric separation of the branes (defined in (80)) must necessarily agree. To check this, the affine distance between the branes is given by

$$\frac{d_a}{L} = \int_{-y_0}^{y_0} n \sqrt{t^2 - t'^2} \, dy \quad (\text{E14})$$

$$= 2 t_0 y_0 + \frac{(t_0 + 5 t_0^3) y_0^3}{3} - 4 t_0^2 y_0^4 + \frac{(t_0 - 10 t_0^3 + 159 t_0^5) y_0^5}{60} - \frac{2 (t_0^2 + 30 t_0^4) y_0^6}{3} + \frac{(t_0 + 31115 t_0^3 - 5523 t_0^5 + 12795 t_0^7) y_0^7}{2520} + O(y_0^8), \quad (\text{E15})$$

which to lowest order in y_0 reduces to

$$\frac{d_a}{L} = 2 x_0 + \frac{5 x_0^3}{3} + \frac{53 x_0^5}{20} + \frac{853 x_0^7}{168} + O(x_0^8) + O(y_0^2), \quad (\text{E16})$$

in agreement with the series expansion of (80). (Note however that the two distance measures differ nontrivially at order y_0^2).

To evaluate the perturbation δd_a in the affine distance between the branes, consider

$$\begin{aligned}\delta \int \sqrt{g_{\mu\nu}\dot{x}^\mu\dot{x}^\nu} d\lambda &= \frac{1}{2} \int \frac{d\lambda}{\sqrt{g_{\rho\sigma}\dot{x}^\rho\dot{x}^\sigma}} (\delta g_{\mu\nu}\dot{x}^\mu\dot{x}^\nu + g_{\mu\nu,\kappa}\delta x^\kappa\dot{x}^\mu\dot{x}^\nu + 2g_{\mu\nu}\dot{x}^\mu\delta\dot{x}^\nu) \\ &= \left[\frac{\dot{x}_\nu\delta x^\nu}{\sqrt{g_{\rho\sigma}\dot{x}^\rho\dot{x}^\sigma}} \right] + \frac{1}{2} \int \frac{\delta g_{\mu\nu}\dot{x}^\mu\dot{x}^\nu}{\sqrt{g_{\rho\sigma}\dot{x}^\rho\dot{x}^\sigma}} d\lambda,\end{aligned}\quad (\text{E17})$$

where dots indicate differentiation with respect to the affine parameter λ , and in going to the second line we have integrated by parts and made use of the background geodesic equation $\ddot{x}_\sigma = \frac{1}{2}g_{\mu\nu,\sigma}\dot{x}^\mu\dot{x}^\nu$ and the constraint $g_{\mu\nu}\dot{x}^\mu\dot{x}^\nu = 1$. If the endpoints of the geodesics on the branes are unperturbed, this expression is further simplified by the vanishing of the surface term. Converting to coordinates where $t_0 = x_0/y_0$ and $y = \omega y_0$, to lowest order in y_0 the unperturbed geodesics lie purely in the ω direction, and so the perturbed affine distance is once again identical to the perturbed metric distance (87).

Explicitly, we find

$$\begin{aligned}\frac{\delta d_a}{L} &= -\frac{2(B + A t_0^2) y_0}{t_0} - \left(\frac{B(4 + 3t_0^2)}{12t_0} + \frac{A(t_0 + 9t_0^3)}{3} \right) y_0^3 + (-4B + 4At_0^2) y_0^4 \\ &\quad - \left(\frac{B(2 + 2169t_0^2 + 135t_0^4) + 2At_0^2(1 + 1110t_0^2 + 375t_0^4)}{120t_0} \right) y_0^5 \\ &\quad + \left(\frac{4At_0^2(1 + 42t_0^2) - B(4 + 57t_0^2)}{6} \right) y_0^6 \\ &\quad - \left(\frac{B(4 + 88885t_0^2 + 952866t_0^4 + 28875t_0^6) + 4At_0^2(1 - 152481t_0^2 + 293517t_0^4 + 36015t_0^6)}{10080t_0} \right) y_0^7 \\ &\quad + O(y_0^8),\end{aligned}\quad (\text{E18})$$

which, substituting $t_0 = x_0/y_0$ and dropping terms of $O(y_0^2)$, reduces to

$$\frac{\delta d_a}{L} = -\frac{2\tilde{B}}{x_0} - 2Ax_0 - \frac{\tilde{B}}{4}x_0 - 3Ax_0^3 - \frac{9}{8}\tilde{B}x_0^3 - \frac{25}{4}Ax_0^5 - \frac{275}{96}\tilde{B}x_0^5 - \frac{343}{24}Ax_0^7 + O(x_0^8), \quad (\text{E19})$$

where $\tilde{B} = By_0^2$. Once again, this expression is in accordance with the series expansion of (87). However, the perturbed affine and metric distances do not agree at $O(y_0^2)$.

[1] P. J. Steinhardt and N. Turok, Phys. Rev. **D65**, 126003 (2002), hep-th/0111098.
[2] J. Khoury, B. A. Ovrut, P. J. Steinhardt, and N. Turok, Phys. Rev. **D64**, 123522 (2001), hep-th/0103239.

- [3] J. Khoury, B. A. Ovrut, N. Seiberg, P. J. Steinhardt, and N. Turok, Phys. Rev. **D65**, 086007 (2002), hep-th/0108187.
- [4] N. Turok, M. Perry, and P. J. Steinhardt, Phys. Rev. **D70**, 106004 (2004), hep-th/0408083.
- [5] L. Randall and R. Sundrum, Phys. Rev. Lett. **83**, 3370 (1999), hep-ph/9905221.
- [6] S. Kanno and J. Soda, Phys. Rev. **D66**, 083506 (2002), hep-th/0207029.
- [7] T. Wiseman, Class. Quant. Grav. **19**, 3083 (2002), hep-th/0201127.
- [8] G. A. Palma and A.-C. Davis, Phys. Rev. **D70**, 064021 (2004), hep-th/0406091.
- [9] L. Randall and R. Sundrum, Phys. Rev. Lett. **83**, 4690 (1999), hep-th/9906064.
- [10] J. Garriga and T. Tanaka, Phys. Rev. Lett. **84**, 2778 (2000), hep-th/9911055.
- [11] S. B. Giddings, E. Katz, and L. Randall, JHEP **03**, 023 (2000), hep-th/0002091.
- [12] M. J. Duff, B. E. W. Nilsson, C. N. Pope, and N. P. Warner, Phys. Lett. **B149**, 90 (1984).
- [13] D. G. Boulware and S. Deser, Phys. Rev. **D6**, 3368 (1972).
- [14] T. Damour and I. I. Kogan, Phys. Rev. **D66**, 104024 (2002), hep-th/0206042.
- [15] R. Brandenberger and F. Finelli, JHEP **11**, 056 (2001), hep-th/0109004.
- [16] F. Finelli and R. Brandenberger, Phys. Rev. **D65**, 103522 (2002), hep-th/0112249.
- [17] D. H. Lyth, Phys. Lett. **B524**, 1 (2002), hep-ph/0106153.
- [18] J.-c. Hwang, Phys. Rev. **D65**, 063514 (2002), astro-ph/0109045.
- [19] J. Hwang and H. Noh, Phys. Lett. **B545**, 207 (2002), hep-th/0203193.
- [20] P. Creminelli, A. Nicolis, and M. Zaldarriaga, Phys. Rev. **D71**, 063505 (2005), hep-th/0411270.
- [21] P. L. McFadden, N. Turok, and P. Steinhardt (to appear).
- [22] D. Langlois, Prog. Theor. Phys. Suppl. **148**, 181 (2003), hep-th/0209261.
- [23] R. Maartens, Living Rev. Rel. **7**, 7 (2004), gr-qc/0312059.
- [24] R. Durrer and F. Vernizzi, Phys. Rev. **D66**, 083503 (2002), hep-ph/0203275.
- [25] A. Lukas, B. A. Ovrut, K. S. Stelle, and D. Waldram, Nucl. Phys. **B552**, 246 (1999), hep-th/9806051.
- [26] A. Lukas, B. A. Ovrut, K. S. Stelle, and D. Waldram, Phys. Rev. **D59**, 086001 (1999), hep-th/9803235.
- [27] Please follow link from <http://wwwphy.princeton.edu/~steinh/>.
- [28] C. van de Bruck, M. Dorca, R. H. Brandenberger, and A. Lukas, Phys. Rev. **D62**, 123515 (2000), hep-th/0005032.
- [29] A. J. Tolley, N. Turok, and P. J. Steinhardt, Phys. Rev. **D69**, 106005 (2004), hep-th/0306109.

- [30] W. Israel, Nuovo Cim. **B44S10**, 1 (1966).
- [31] R. M. Corless, G. H. Gonnet, D. E. G. Hare, D. J. Jeffrey, and D. E. Knuth, Adv. Comp. Math. pp. 329–359 (1996), see also <http://mathworld.wolfram.com/LambertW-Function.html>.
- [32] Note that the radius of convergence of the series (45) for $W(x)$ is $1/e$, and thus it converges for arguments in the range $-1/e \leq x \leq 0$ as required.
- [33] From the exact solution in bulk-static coordinates, the scale factor on the negative-tension brane at the horizon obeys $b_-^2 = \text{sech}^2 Y_0/L = \tanh y_0$, and so $b_- \sim y_0^{1/2}$.
- [34] C. Csaki, M. Graesser, L. Randall, and J. Terning, Phys. Rev. **D62**, 045015 (2000), hep-ph/9911406.
- [35] J. Khoury and R.-J. Zhang, Phys. Rev. Lett. **89**, 061302 (2002), hep-th/0203274.
- [36] P. L. McFadden and N. Turok, Phys. Rev. **D71**, 021901 (2005), hep-th/0409122.
- [37] V. F. Mukhanov, H. A. Feldman, and R. H. Brandenberger, Phys. Rept. **215**, 203 (1992).
- [38] J. M. Bardeen, Phys. Rev. **D22**, 1882 (1980).
- [39] J. Khoury, B. A. Ovrut, P. J. Steinhardt, and N. Turok, Phys. Rev. **D66**, 046005 (2002), hep-th/0109050.
- [40] In a companion paper [21] we show that A_4^L is in fact proportional to ζ , the comoving curvature perturbation on the positive-tension brane, which is conserved on long wavelengths.
- [41] P. L. McFadden and N. G. Turok, Phys. Rev. **D71**, 086004 (2005), hep-th/0412109.
- [42] A. Chamblin, S. W. Hawking, and H. S. Reall, Phys. Rev. **D61**, 065007 (2000), hep-th/9909205.